Inorganic Chemistry

Article

pubs.acs.org/IC

Magnesium and Calcium Complexes Containing Biphenyl-Based Tridentate Iminophenolate Ligands for Ring-Opening Polymerization of *rac*-Lactide

Wei Yi and Haiyan Ma*

Shanghai Key Laboratory of Functional Materials Chemistry and Laboratory of Organometallic Chemistry, East China University of Science and Technology, 130 Meilong Road, Shanghai 200237, People's Repulbic of China

Supporting Information

ABSTRACT: A series of racemic 2-[(2′-methoxybiphenyl-2-ylimino)methyl]-4-R^2-6-R^1-phenols ($\mathbf{L^1H}$-$\mathbf{L^8H}$) were reacted with $\{Mg[N(SiMe_3)_2]_2\}_2$ and $Ca[N(SiMe_3)_2]_2$·2THF (THF = tetrahydrofuran), respectively, to provide nine heteroleptic magnesium complexes $\mathbf{L^{1-8}}MgN(SiMe_3)_2$ [R^1 = ^{i}Pr, R^2 = H (**1a**); R^1 = ^{t}Bu, R^2 = Me (**2a** and **2a**·THF); R^1 = R^2 = ^{t}Bu (**3a**); R^1 = R^2 = CMe_2Ph (**4a**); R^1 = CPh_3, R^2 = ^{t}Bu (**5a**); R^1 = 1-piperidinylmethyl, R^2 = ^{t}Bu (**6a**); R^1 = Cl, R^2 = ^{t}Bu (**7a**); R^1 = Br, R^2 = ^{t}Bu (**8a**)], two homoleptic calcium complexes $(\mathbf{L^{2,5}})_2Ca$ (**2b** and **5b**), and one heteroleptic calcium complex $[(\mathbf{L^4})CaN(SiMe_3)_2$·THF] (**4b**), which have been fully characterized. In the solid state, magnesium complexes **2a** and **6a** are isostructural, and each possesses a monomeric structure, while magnesium complexes **7a** and **8a** are dimeric, where the two metal centers are bridged by two phenolate oxygen atoms of the ligands. The coordination geometry around the magnesium center in these complexes can be best described as a distorted tetrahedral geometry. Although bearing the same iminophenoloate ligand, the molecular structures of complexes **2a** and **2a**·THF are different from each other. In complex **2a**·THF, the coordination of one molecule of THF to the magnesium atom leads to dissociation of the methoxy group of the ligand from the metal center. The homoleptic calcium complex **2b** has a six-coordinate metal core ligated by all six donor atoms of two iminophenolate ligands. The heteroleptic magnesium complexes **1a**−**8a** and calcium complex **4b** proved to be efficient initiators for the ring-opening polymerization of *rac*-lactide at ambient temperature in THF or at 70 °C in toluene, and the polymerizations were better controlled in the presence of 2-propanol. The introduction of a bulky ortho substituent on the phenoxy unit of the ligand resulted in an increase of the catalytic activity of the corresponding metal complex. Microstructure analysis of the resultant poly(*rac*-lactide) samples via homonuclear-decoupled ^{1}H NMR spectroscopy revealed P_r values ranging from 0.60 to 0.81, which closely depended on the employed catalyst and polymerization conditions.

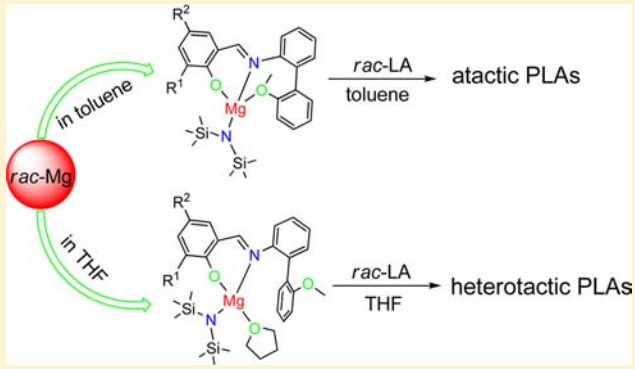

INTRODUCTION

Polylactides (PLAs) as biodegradable and biocompatible materials have been widely used in the biomedical and pharmaceutical fields and more recently are considered as environmentally friendly alternatives to olefinic polymers.[1] Accordingly, the preparation of PLA has been drawn intensive scrutiny, and the use of metal-based catalysts for the ring-opening polymerization (ROP) of lactides (LAs) proves to be the most effective.[2] Many discrete complexes of various metals, such as aluminum,[3] indium,[4] tin,[5] sodium,[6] zinc,[7] magnesium,[8] calcium,[9] titanium, zirconium,[10] and rare-earth metals,[11] have been synthesized and evaluated for this issue. Although a large variety of metal derivatives could effectively catalyze the ROP of LAs, it is preferable to use initiators based on biocompatible metals such as magnesium and calcium because PLAs are more widely utilized as surgical sutures,[12] drug-delivery vehicles,[13] and artificial tissue matrices.[14]

Alkaline-earth metal complexes supported by iminophenoloate ligands have been used as catalysts in many applications because of the diverse forms and easy preparation of iminophenol proligands.[15] The first magnesium iminophenolate complex $[(SalenOMe)Mg(OBn)]_2$ used as an initiator for the polymerization of *rac*-LA was developed by Lin and co-workers.[16] The complex exhibited good catalytic activity and yielded PLAs with very narrow molecular weight distributions. However, it only afforded heterotactic bias PLAs (P_r = 0.57) in tetrahydrofuran (THF) and atactic polymers in toluene at room temperature. Recently, the same group[17] also reported a series of magnesium complexes supported by NNO-tridentate iminophenolate ligands for the ROP of L-LA. The results showed that the introduction of an electron-withdrawing substituent at the para position of the phenoxy unit decreased

Received: May 22, 2013
Published: October 1, 2013

Scheme 1. [a]

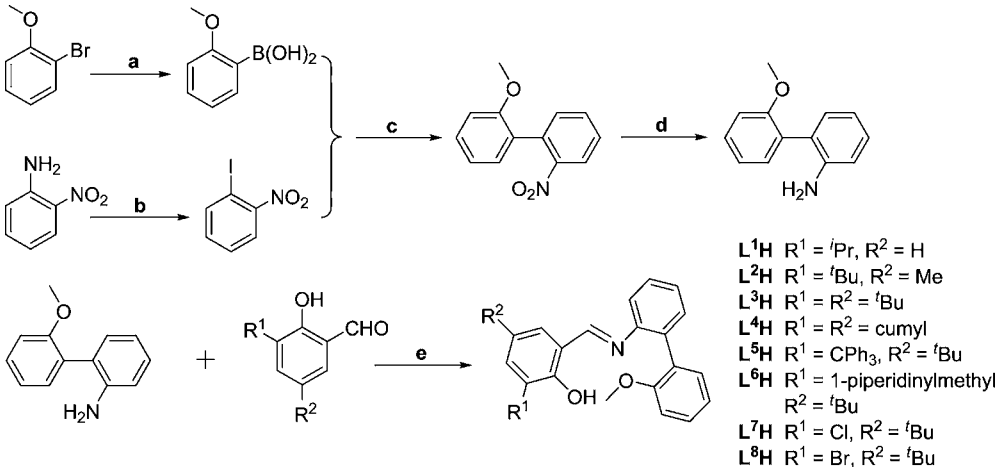

[a](a) (1) −78 °C, *n*-BuLi/$B(OMe)_3$; (2) HCl. (b) −5 to 0 °C, $HCl/NaNO_2/KI$. (c) $PdCl_2(PPh_3)_2/K_2CO_3/^iPrOH$; 12 h. (d) Sn/HCl, ethanol, reflux 5 h. (e) ethanol, reflux, 5h.

Scheme 2

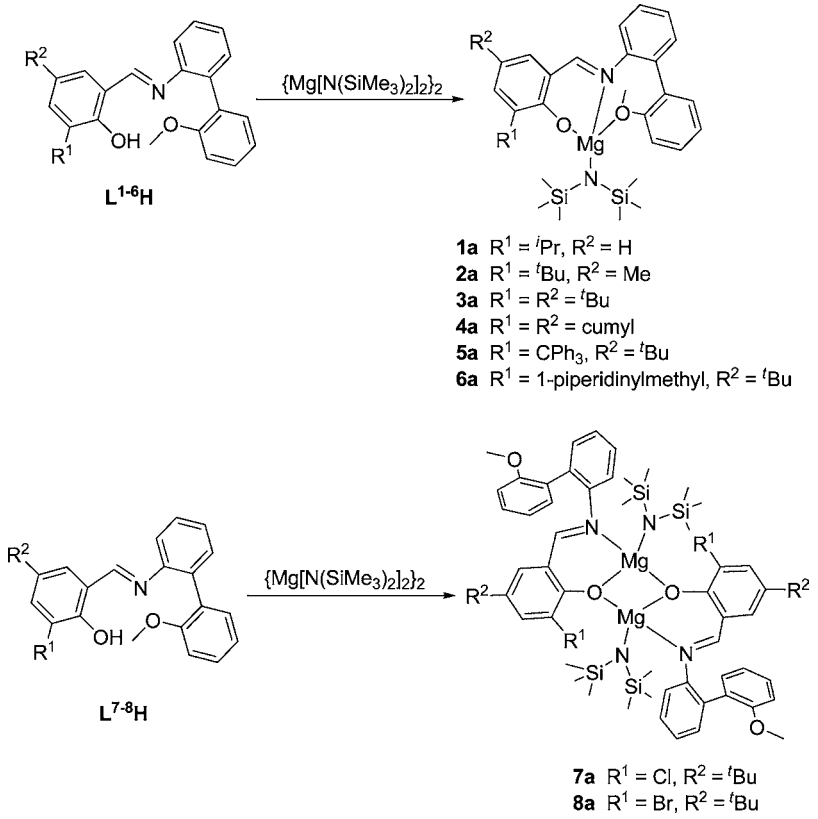

the catalytic activity of the corresponding complex. More recently, Darensbourg and Karroonnirun[7j] assessed a zinc silylamido complex supported by chiral NNO-tridentate iminophenolate ligand for the polymerization of *rac*-LA in dichloromethane (DCM), and predominantly heterotactic PLAs (P_r = 0.68−0.89) were obtained. Unfortunately, analogous magnesium and calcium complexes ligated with the same ligand are not reported. By looking into the structure of the mentioned chiral zinc silylamido complex, we find that the chiral unit is far away from the zinc center, which might not be capable of inducing a specific chirality at the metal center. Biphenyl derivants are widely used in asymmetric synthesis.[18] It is considerable that the axial chirality of the biphenyl framework may serve as an excellent chiral resource to induce a specific chirality at the metal center of the target complex, and when it is used in racemic form, the resultant racemic complex would be more favorable for the stereoselective ROP of *rac*-LA. Herein we describe the preparation of a series of magnesium and calcium complexes supported by novel tridentate imonophenolate ligands based on a racemic biphenyl framework. The catalytic performances of the silylamido complexes toward the ROP of *rac*-LA are reported in detail.

dx.doi.org/10.1021/ic4012668 | *Inorg. Chem.* 2013, 52, 11821−11835

Scheme 3

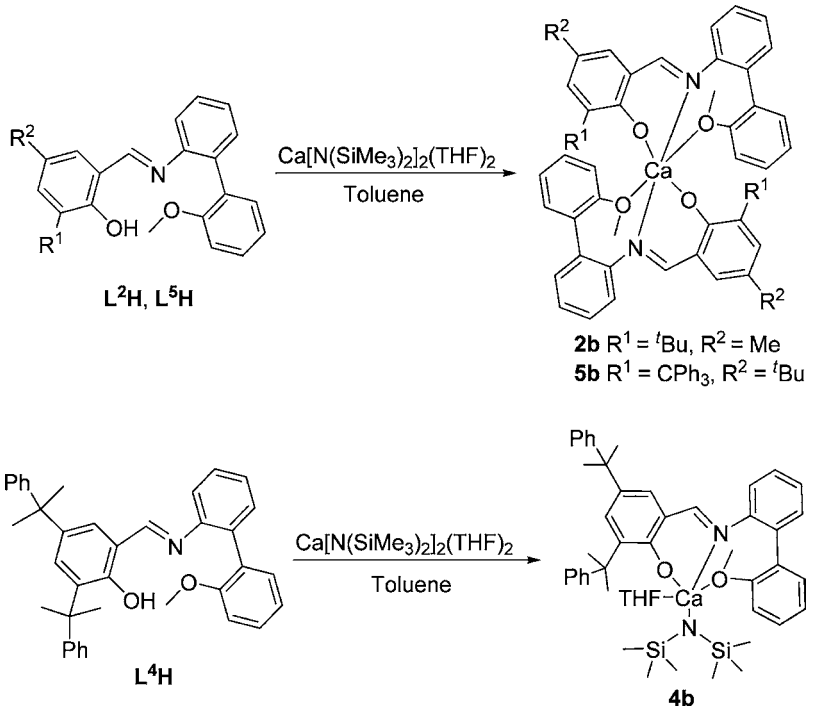

RESULTS AND DISCUSSION

Synthesis and Characterization of Magnesium and Calcium Complexes. Scheme 1 illustrates the synthetic strategies to prepare the desired biphenyl-based iminophenol proligands. The synthesis of 2-methoxy-2′-nitrobiphenyl was based on a modified procedure reported in the literature.[19] Via a Suzuki coupling reaction between 1-iodo-2-nitrobenzene and 2-methoxyphenylboronic acid, the mentioned compound could be isolated in high yield of 94%. 2′-Methoxybiphenyl-2-amine was obtained by a reduction of the above coupling product in the existence of tin. Condensation reactions of this amine with different substituted salicylaldehyde derivatives under reflux in ethanol yielded the target biphenyl-based iminophenol proligands $\mathbf{L^{1-8}H}$. All of the obtained iminophenols except for $\mathbf{L^4H}$ are yellow-to-orange crystalline solids, whereas $\mathbf{L^4H}$ is isolated as an orange viscous oil. All proligands were characterized via ^{1}H and ^{13}C{^{1}H} NMR spectroscopy and high-resolution mass spectroscopy (HRMS).

The heteroleptic magnesium complexes **1a**−**8a** were prepared in moderate yields from the reaction of {Mg[N(SiMe$_3$)$_2$]$_2$}$_2$ and 1 equiv of the corresponding proligand in toluene at room temperature, respectively (Scheme 2). The recrystallization process accounting for further purification was somewhat challenging because these complexes are highly soluble in toluene or THF but almost insoluble in *n*-hexane. Finally, all of the magnesium complexes were successfully recrystallized in a mixture of toluene/*n*-hexane at room temperature or at −38 °C to give yellow-green crystalline solids. For all complexes, the spectroscopic data and elemental analysis are consistent with the stoichiometric structure of one iminophenolate ligand and one bis(trimethylsilyl)amido group chelating to the metal center. Although there exist both an axially chiral biphenyl moiety and a stereogenic metal center in each complex, no diastereomer could be observed in the ^{1}H NMR spectra of these complexes, suggesting that the axial chirality of biphenyl may have induced exclusively a certain configuration at the magnesium center. As shown in the following figures (vide post), in the solid state complexes **1a**−**6a** are monomeric, while complexes **7a** and **8a** with *o*-halogen substitution each possess a dimeric structure. Attempts at recrystallization of magnesium complex **2a** with a THF/*n*-hexane mixture afforded a THF-coordinated magnesium complex, **2a**·THF, as pale-yellow needlelike crystals, which was also characterized via X-ray diffraction study to be monomeric.

Similar reactions of selected proligands $\mathbf{L^2H}$, $\mathbf{L^4H}$, and $\mathbf{L^5H}$ with Ca[N(SiMe$_3$)$_2$]$_2$·2THF were carried out to synthesize the corresponding calcium silylamido complexes. Unexpectedly, the reaction of equimolar amounts of $\mathbf{L^2H}$ and Ca[N(SiMe$_3$)$_2$]$_2$·2THF did not give the target heteroleptic calcium complex ($\mathbf{L^2}$)CaN(SiMe$_3$)$_2$, but the bisligated complex ($\mathbf{L^2}$)$_2$Ca (**2b**) isolated in moderate yield. Therefore, the reaction of $\mathbf{L^2H}$ with an excess of Ca[N(SiMe$_3$)$_2$]$_2$·2THF in a ratio of 1:1.5 was monitored via ^{1}H NMR spectroscopy, which indicated that the bisligated calcium complex **2b** was formed immediately after the mix of two reactants (less than 30 min) accompanied by the release of 2 equiv of free HN(SiMe$_3$)$_2$ (Figure S1 in the Supporting Information, SI). No signal assignable to the target heteroleptic calcium complex could be observed, suggesting that the formation of **2b** did not arise from a rearrangement upon workup. Further attempts in carrying the reaction at −78 °C throughout did not move the equilibrium to the heteroleptic product. Complex **2b** could also be quantitatively prepared from the reaction of $\mathbf{L^2H}$ and Ca[N(SiMe$_3$)$_2$]$_2$·2THF in a molar ratio of 2:1. Such behavior was in stark contrast with that of the reaction between $\mathbf{L^4H}$ and Ca[N(SiMe$_3$)$_2$]$_2$·2THF, which readily led to the formation of the corresponding heteroleptic complex ($\mathbf{L^4}$)CaN(SiMe$_3$)$_2$·THF (**4b**; Scheme 3). To prove whether it is due to a steric effect of the ortho substituent on the phenoxy ring, the reaction of $\mathbf{L^5H}$ (bearing an *o*-trityl group) and Ca[N(SiMe$_3$)$_2$]$_2$·2THF was conducted, which, however, led to the bisligated calcium complex **5b**

dx.doi.org/10.1021/ic4012668 | Inorg. Chem. 2013, 52, 11821−11835

beyond our expectation. It seems that a much more complicated situation is encountered, where the steric/electronic effects of the ligand substituents as well as solubility differences between the homolepic and heterolepic complexes may contribute together to the formation of one specific product.

All of these magnesium and calcium complexes have been fully characterized, and their structures in solution were investigated in detail via ^{1}H NMR spectroscopy with the aim of understanding the coordination environment around the metal center. As shown in Table 1, the resonance of the methoxy protons of magnesium complex **1a** appears at 3.61 ppm in the ^{1}H NMR spectrum, which is 0.27 ppm downfield-shifted from that of the free ligand $\mathbf{L^1H}$ (3.34 ppm). A similar situation could also be found for magnesium complexes **2a**–**6a** and calcium complex **4b**, which proves that in solution these complexes are monomeric and the methoxy group of the iminophenolate ligand in these complexes is still coordinated to the metal center. This assignment is also supported by X-ray diffraction analyses of **2a** and **6a**.

Table 1. Chemical Shifts of Methoxy Resonances in the ^{1}H NMR Spectra of Magnesium Complexes and Corresponding Proligands[a]

	Ar-OCH_3			Ar-OCH_3
complex	C_6D_6	C_6D_6 with THF[b]	ligand	C_6D_6
1a	3.61	3.33	$\mathbf{L^1H}$	3.34
2a	3.57	3.28[c]	$\mathbf{L^2H}$	3.35
3a	3.59	3.33	$\mathbf{L^3H}$	3.37
4a	3.45	3.09	$\mathbf{L^4H}$	3.16
5a	3.40	3.35	$\mathbf{L^5H}$	3.10
6a	3.65	3.47	$\mathbf{L^6H}$	3.35
7a	3.61[d]	3.39	$\mathbf{L^7H}$	3.37
8a	3.62	3.29	$\mathbf{L^8H}$	3.37

[a]In ppm. [b]One tiny drop of THF was added to the solution of the magnesium complex in C_6D_6. [c]The corresponding resonance of complex **2a**·THF in C_6D_6. [d]The corresponding resonance of the major structure in C_6D_6.

Two sets of signals accounting for the stoichiometric structure are displayed in the ^{1}H NMR spectrum of **7a** in benzene-d_6, represented by the methoxy resonances at 3.61 and 3.29 ppm (with a ratio of 4:1). It is worth noting that, although the X-ray diffraction determination indicates a dimeric structure of complex **7a** in the solid state where the methoxy group of the biphenyl moiety is not coordinated to the magnesium center, a significant downfield shift of the methoxy resonance attributable to the major structure is also observed compared to that of the free ligand. The relevant resonance of the minor structure, however, resembles the one of the free ligand. Similar features are also observed in the ^{1}H NMR spectrum of **8a** in toluene-d_8 at 25 °C (Figure S2a in the SI). With an increase of the temperature from 25 to 105 °C, the broad signals of the minor structure of **8a** disappeared completely above 75 °C. In the low-temperature region (−60 to +20 °C), no significant increase of the signals of the minor structure with a decrease of the temperature could be observed (Figure S2b in the SI); instead, a very small amount of a new structure with a CH_3O– chemical shift at 3.04 ppm and a $N[Si(CH_3)_3]_2$ resonance at 0.15 ppm appeared below −40 °C. It is, therefore, suggested that the dominant structures of **7a** and **8a** in solution are still monomeric and the minor isomer should have a dimeric structure. As to the third structure of **8a** appearing below −40 °C, probably it is a diastereomer of the minor isomer.

The singlet of the methoxy protons of magnesium complex **2a**·THF appears at 3.28 ppm, which is upfield-shifted from that of complex **2a** (3.57 ppm) and is closer to the corresponding resonance of the free ligand $\mathbf{L^2H}$, indicating that the coordination of THF leads to dissociation of the methoxy group in **2a**·THF. Darensbourg and co-workers[7j] also declaimed that the structure of a zinc diaminophenolate complex is different in a coordinative solvent or not. To examine the universality in this series of complexes, we measured the ^{1}H NMR spectra of the rest of the magnesium complexes in benzene-d_6 with the addition of one tiny drop of THF (around 1–3 equiv). As expected, a significant upfield shift of the methoxy resonance could be observed for most of the complexes, suggesting that the methoxy group is dissociated from the magnesium center in the presence of THF. Complex **5a** showed a different situation, where the resonance of the methoxy protons is hardly shifted. Likely, the methoxy group is still coordinated to the metal center, probably because of protection by the bulky *o*-trityl group.

Crystal Structures of Magnesium Complexes 2a, 2a·THF, 6a, 7a, and 8a and Calcium Complex 2b. Complexes **2a**, **2a**·THF, **6a**, **7a**, **8a**, and **2b** were further characterized by single-crystal X-ray diffraction studies. The single crystals were obtained by slightly cooling a saturated toluene/*n*-hexane mixture or a THF/*n*-hexane mixture, respectively. Crystallographic data and results of the refinements are summarized in Table S1 in the SI, and selected bond lengths and angles are listed in Tables 2 and 3.

As depicted in Figure 1, complex **2a** has a monomeric structure in the solid state where the magnesium atom is four-coordinated by three heteroatom donors of the tridentate ligand and one bis(trimethylsilyl)amido group, adopting a distorted tetrahedral geometry. The molecule shows C_1 symmetry, and both enantiomers are found in the centrosym-

Table 2. Selected Bond Lengths (Å) and Angles (deg) in 2a, 2a·THF, and 6a

	[($\mathbf{L^2}$)MgN($SiMe_3$)$_2$·toluene] (**2a**)		
Mg1–O2	1.889(4)	Mg1–N1	1.985(4)
Mg1–O1	2.062(4)	Mg1–N2	2.106(4)
O2–Mg1–N1	119.75(18)	O2–Mg1–O1	120.80(16)
N1–Mg1–O1	105.64(16)	O2–Mg1–N2	89.54(16)
N1–Mg1–N2	131.84(17)	O1–Mg1–N2	86.45(15)
	[($\mathbf{L^2}$)MgN($SiMe_3$)$_2$·THF] (**2a**·THF)		
Mg1–O1	1.9109(17)	Mg1–N2	1.987(2)
Mg1–O3	2.025(2)	Mg1–N1	2.097(2)
Si1–N2	1.702(2)	Si2–N2	1.693(2)
O1–Mg1–N2	123.80(8)	O1–Mg1–O3	96.93(8)
N2–Mg1–O3	114.66(9)	O1–Mg1–N1	90.65(7)
N2–Mg1–N1	118.41(9)	O3–Mg1–N1	108.35(8)
Si2–N2–Si1	125.00(12)		
	[($\mathbf{L^6}$)MgN($SiMe_3$)$_2$] (**6a**)		
Mg1–O1	1.905(2)	Mg1–N3	1.985(3)
Mg1–O2	2.047(2)	Mg1–N1	2.111(3)
O1–Mg1–N3	117.35(11)	O1–Mg1–O2	120.40(11)
N3–Mg1–O2	103.37(11)	O1–Mg1–N1	88.55(10)
N3–Mg1–N1	136.79(11)	O2–Mg1–N1	89.76(10)

dx.doi.org/10.1021/ic4012668 | Inorg. Chem. 2013, 52, 11821–11835

Table 3. Selected Bond Lengths (Å) and Angles (deg) in 7a, 8a, and 2b

	[(L^7)MgN(SiMe$_3$)$_2$] (**7a**)		
Mg1−O2	1.9953(18)	Mg1−O1	1.9981(18)
Mg1−N3	2.000(2)	Mg1−N1	2.143(2)
Mg2−N4	1.994(2)	Mg2−O1	1.9935(18)
Mg2−N2	2.139(2)	Mg2−O2	2.0016(19)
O2−Mg1−O1	80.05(7)	O2−Mg1−N3	131.11(9)
O1−Mg1−N3	127.03(9)	O2−Mg1−N1	111.33(8)
O1−Mg2−N4	130.87(9)	O1−Mg2−O2	80.01(7)
N4−Mg2−O2	125.41(9)	O1−Mg2−N2	108.23(8)
	[(L^8)MgN(SiMe$_3$)$_2$] (**8a**)		
Mg1−O2	1.993(4)	Mg1−O1	1.999(4)
Mg1−N3	1.998(5)	Mg1−N1	2.150(5)
Mg2−N2	2.151(5)	Mg2−O1	2.000(4)
Mg2−N4	2.000(5)	Mg2−O2	2.004(4)
O2−Mg1−O1	79.52(15)	O2−Mg1−N3	129.58(18)
O1−Mg1−N3	124.46(19)	O2−Mg1−N1	111.51(17)
O1−Mg2−N4	129.11(18)	O1−Mg2−O2	79.22(15)
N4−Mg2−O2	127.31(19)	O1−Mg2−N2	114.23(17)
	[(L^2)$_2$Ca] (**2b**)		
Ca1−O2	2.410(5)	Ca1−N1	2.472(6)
Ca1−N2	2.481(6)	Ca1−O4	2.553(6)
Ca1−O3	2.184(5)	Ca1−O1	2.203(5)
O1−Ca1−O2	115.9(2)	O3−Ca1−N1	160.4(2)
O1−Ca1−N1	74.46(19)	O2−Ca1−N1	77.05(19)
O2−Ca1−N2	88.1(2)	O2−Ca1−O4	148.56(19)
O3−Ca1−O4	108.09(18)	O1−Ca1−O4	88.01(19)

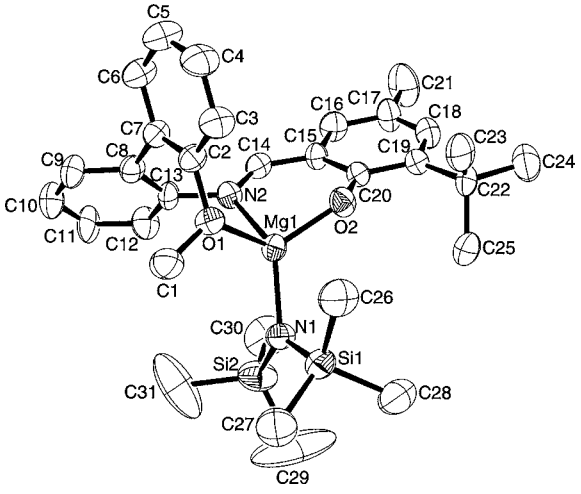

Figure 1. ORTEP diagram of the molecular structure of **2a**. Thermal ellipsoids are drawn at the 30% probability level. Hydrogen atoms are omitted for clarity.

metric crystal structure. Without exception, the R_a configuration of the biphenyl moiety in the iminophenolate ligand leads to an *S* configuration of the magnesium center, and vice versa S_a leads to an *R* configuration. The bond length between the magnesium atom and silylamido nitrogen atom (Mg1−N1) in complex **2a** is 1.985(4) Å, which is in the normal range of 1.980−2.023 Å reported in the literature.[10d,20] The dihedral angle of the biphenyl moiety being 57.6°, obviously smaller than that of the free ligand,[21] is likely due to coordination of the methoxy group to the magnesium center. The molecular structure of complex **2a**·THF (Figure 2) is different from that

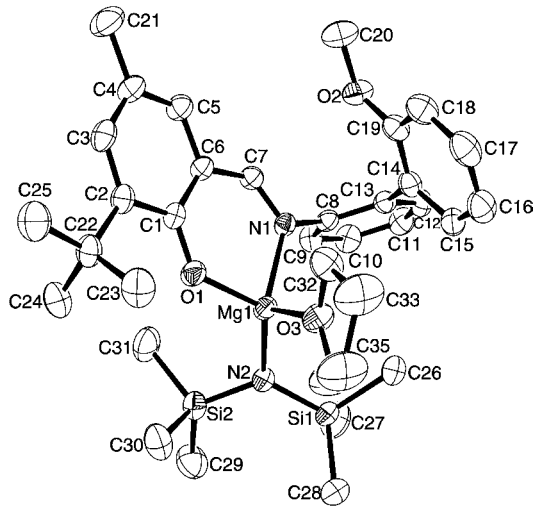

Figure 2. ORTEP diagram of the molecular structure of **2a**·THF. Thermal ellipsoids are drawn at the 30% probability level. Hydrogen atoms are omitted for clarity.

of complex **2a**, with the oxygen atom of the methoxy group in **2a**·THF dissociating from the metal center. In complex **2a**·THF, the magnesium atom is still four-coordinated by two heteroatom donors of the tridentate ligand, one bis(trimethylsilyl)amido group, and one molecule of THF, adopting a distorted tetrahedral geometry, instead of a five-coordinate structure usually adopted by common magnesium complexes.[20a,22] More interestingly, it is found that, in complex **2a**·THF, the R_a configuration of the biphenyl moiety in the iminophenolate ligand leads to an *R* configuration of the magnesium center instead, which is in contrast to the situation in **2a**. It seemed that, during the recrystallization process of **2a** with THF, the coordinated methoxy group in **2a** was substituted by a THF molecule via a "S_N2"-type reaction to afford a reversed configuration at the metal center. Furthermore, as expected the dihedral angle of the biphenyl moiety in complex **2a**·THF is 70.82°, obviously larger than that of complex **2a**.

The molecular structure of complex **6a** (Figure 3) is similar to that described for complex **2a**. The introduction of an additional donor atom in the piperidinyl group hardly influences the coordination geometry in complex **6a** because the N2 atom of piperidinyl is located far away and not coordinated to the magnesium center. In addition, the angle of N3−Mg−N1 = 136.79(11)° in complex **6a** is significantly more open than that in complex **2a** [131.84(17)°]. A slightly larger dihedral angle of biphenyl (60.02°) than that of **2a** is also observed. Similar to **2a**, the R_a configuration of the biphenyl moiety in **6a** also leads to an *S* configuration of the magnesium center or vice versa.

The ORTEP drawing of the molecular structure of **7a** given in Figure 4 shows that in the solid state complex **7a** possesses a dimeric structure with two metal centers bridged by the two phenolato oxygen atoms of the ligands, and the whole molecule has C_1 symmetry, as indicated by slight differences in the corresponding bond lengths and angles. Each magnesium center adopts a distorted tetrahedral geometry. The methoxy groups of both iminophenolate ligands are not coordinated to

dx.doi.org/10.1021/ic4012668 | *Inorg. Chem.* 2013, 52, 11821−11835

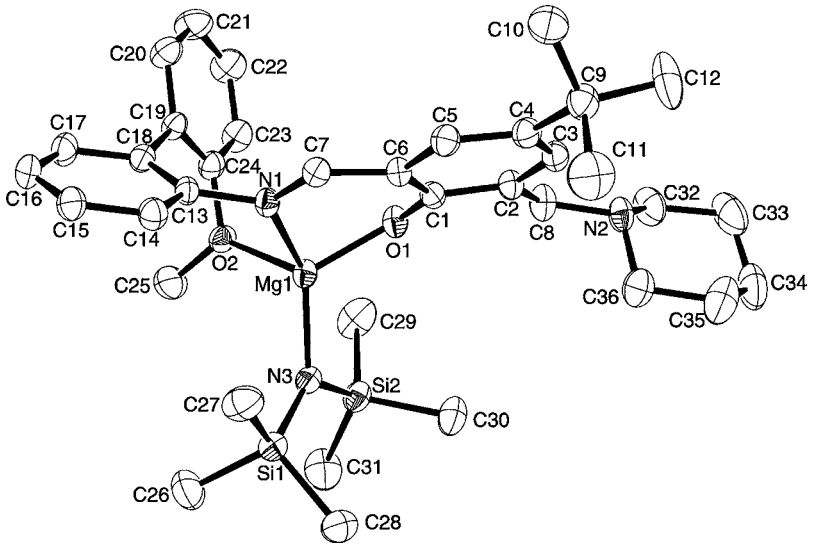

Figure 3. ORTEP diagram of the molecular structure of **6a**. Thermal ellipsoids are drawn at the 30% probability level. Hydrogen atoms are omitted for clarity.

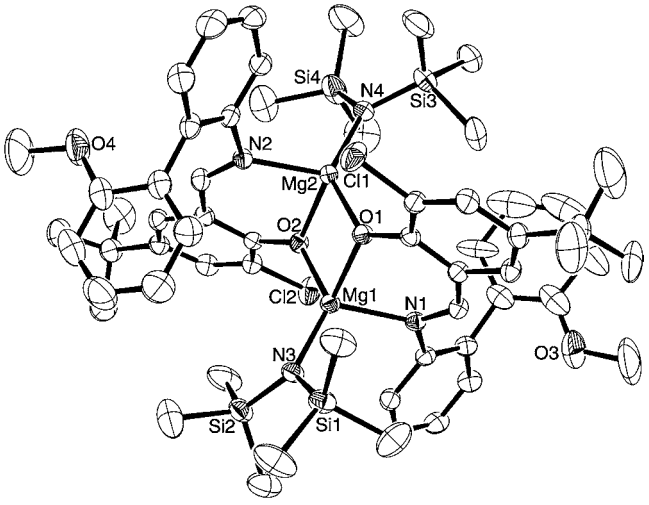

Figure 4. ORTEP diagram of the molecular structure of **7a**. Thermal ellipsoids are drawn at the 30% probability level. Hydrogen atoms are omitted for clarity.

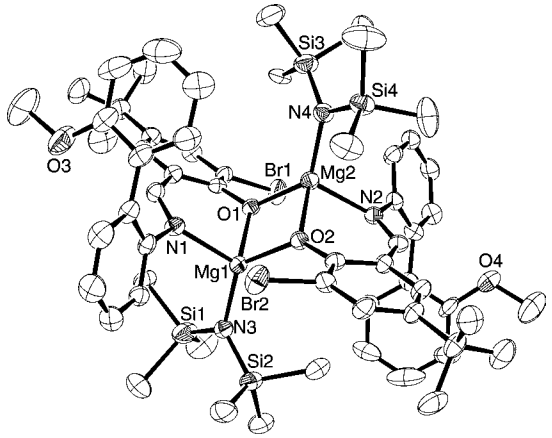

Figure 5. ORTEP diagram of the molecular structure of **8a**. Thermal ellipsoids are drawn at the 30% probability level. Hydrogen atoms are omitted for clarity.

magnesium centers. Both magnesium centers are still chiral because the biphenyl moieties of two ligands possess opposite chiral configurations. The Mg–N (silylamido) bond lengths in complex **7a** [Mg1–N3 = 2.000(2) Å; Mg2–N4 =1.994(2) Å] are longer than that in complex **2a** [1.985(4) Å] but still in the normal range reported in the literature (1.980–2.023 Å).[10d,20] The Mg2–O1–Mg1 angle is about 100.05(8)°, and the distance of Mg···Mg is 3.0588(12) Å, slightly longer than the reported values for $[(SalenMe)Mg(OBn)]_2$[16] (2.999 Å). Similar to complex **2a**·THF, the dihedral angles of the biphenyl moieties in **7a** being 74.82° and 74.44° are also larger than those of **2a** and **6a** with a coordinated methoxy group. The solid-state structure of complex **8a** (Figure 5) is shown to be similar, which is also dimeric. Each magnesium center adopts a distorted tetrahedral geometry, and the configurations of two biphenyl moieties in one molecule are mainly opposite.[23] Significantly larger dihedral angles of the biphenyl units in **8a** (82.70° and 75.55°) than those of all of the other complexes are observed. It is worth noting that, in complexes **7a** and **8a**, two corresponding magnesium–halogen distances deviate from each other significantly (Mg1–Cl2 = 3.862 Å vs Mg2–Cl1 = 3.538 Å for **7a**; Mg1–Br2 = 3.469 Å vs Mg2–Br1 = 3.871 Å for **8a**), probably indicating somewhat weak van der Waals interaction between one magnesium center and a halogen atom, especially for **8a** with a Mg1–Br2 distance shorter than the sum of the metal radius r_m(Mg) and the van der Waals radius r_v(Br) [r_m(Mg) + r_v(Br) = 1.60 + 2.00 = 3.60 Å]. Likely, it is the van der Waals force that breaks the symmetry of the molecule.

As shown in Figure 6, calcium complex **2b** possesses a monomeric structure in the solid state and has a six-coordinate calcium core, adopting a distorted octahedral geometry. The whole molecule shows C_1 symmetry, with the two biphenyl moieties possessing the same axial chirality. The distances between the calcium atom and O1 and O3 of two phenoxy units are 2.203(5) and 2.184(5) Å, respectively. The angle of O3–Ca1–N1 being 160.4(2)° is the largest, and thus O3, Ca1, and N1 construct the axis of the octahedral structure. The other donor atoms of O1, O2, O4, and N2 are in the equatorial position. The distance between the calcium atom and the (O1,

dx.doi.org/10.1021/ic4012668 | Inorg. Chem. 2013, 52, 11821–11835

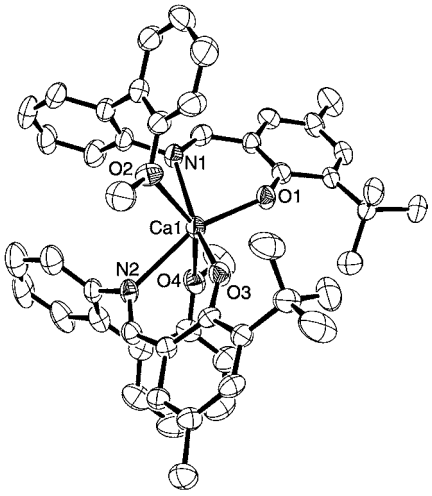

Figure 6. ORTEP diagram of the molecular structure of **2b**. Thermal ellipsoids are drawn at the 30% probability level. Hydrogen atoms are omitted for clarity.

O2, and N2) plane is 0.034 Å. The O2 and O4 atoms of two methoxy groups are in the reverse positions, as indicated by the corresponding angle of O2−Ca−O4 = 148.56(19)°.

ROP of *rac*-LA. All of the synthesized magnesium complexes **1a**−**8a** and calcium complexes **2b**, **4b**, and **5b** were evaluated as initiators for the ROP of *rac*-LA in THF at room temperature or in toluene at 70 °C. The representative polymerization data are summarized in Table 4. Except for the homoleptic calcium complexes **2b** and **5b**, all of these alkaline-earth silylamido complexes can effectively initiate the ROP of *rac*-LA either alone or in the presence of 2-propanol, giving PLAs with high molecular weights and relatively broad molecular weight distributions (M_w/M_n = 1.06−1.75).

The structure of the ancillary ligand has a considerable influence on the catalytic performance of the corresponding metal complex. For instance, magnesium complex **5a** with an *o*-trityl group on the phenolate ring displayed the highest catalytic activity among this series of magnesium complexes. The polymerization went to 94% monomer conversion in 1.5 min at room temperature in THF (entry 17), whereas the rest of the complexes achieved moderate-to-high monomer conversions within 30 min under otherwise identical polymerization conditions. A general increasing tendency of catalytic activity with an increase of the steric bulkiness of the ortho substituent on the phenolate ring could be observed for magnesium complexes **1a**−**5a**, that is, **5a** (CPh_3) > **4a** (cumyl) > **3a** (^{t}Bu) ≈ **2a** (^{t}Bu) > **1a** (^{i}Pr). Lin et al.[24] reported that by replacing 1,5-dimethyl groups with steric bulkier *tert*-butyl groups in the tridentate *β*-ketiminatomagnesium alkoxide complexes [LMg-(μ-OBn)]$_2$, the catalytic activity of the resultant complex increased dramatically. Recently, Okuda and co-workers[10i] also reported a series of group 4 metal complexes containing bridged bis(phenolate) ligands of the (OSSO) type; it was founded that the complex with a bulky *o*-cumyl group displayed higher activity for *meso*-LA polymerization than the one with an *o*-*tert*-butyl group. All of these can be attributed to the fact that the introduction of steric bulkier groups, especially at the ortho position of the anionic donor atom (in this work, the phenoxide), could protect more efficiently the metal center of active metal alkoxide species from aggregation and therefore lead to an increase of the catalytic activity. In comparison with magnesium complexes **1a**−**5a**, magnesium complex **6a** with an *o*-piperidinylmethyl substituent displayed a relatively lower activity, which might be ascribed to the existence of an additional donor group in the piperidinyl ring, unfavorable for the coordination/insertion of monomer. Complexes **7a** and **8a** with an *o*-halogen substituent on the phenolate ring also displayed lower activities. A similar effect was previously reported for magnesium complexes supported by NNO-tridentate iminophenolate[17] or *β*-ketiminato[24] ligands, where the electron-withdrawing group was substituted at the para position of the phenolate ring or the 1 position of the ketiminato framework. The authors suggested that the introduction of an electron-withdrawing group caused the magnesium atom to be more acidic, resulting in a stronger Mg−OR bond during polymerization, which retarded the insertion reaction of monomer. It is therefore conceivable that the electronic-withdrawing effect of an *o*-halogen substituent in complexes **7a** and **8a** may also play a dominant role during polymerization. Besides, on the basis of the fact that a dimeric structure is even obtained for magnesium silylamido complexes **7a** and **8a** in the solid state, the steric effect of a smaller *o*-halogen group in **7a** and **8a**, which is not sufficient to prevent the active magnesium center (in the Mg−OR form during polymerization) from aggregating, could not be ruled out.

To investigate the exact influence of ligand substituents on the polymerization rate of *rac*-LA, preliminary kinetic studies were carried out for representative magnesium complexes with an initiator/monomer ratio of 1:25 ($[LA]_0$ = 0.20 mol·L^{-1}) at 25 °C in benzene-d_6. The semilogarithmic plots of ln($[LA]_0$/$[LA]_t$) versus time are presented in Figure 7. A clear decreasing tendency of the apparent propagation rate is observed in the order of **5a** (CPh_3; k_{obs} = 0.11 min^{-1}) > **4a** (cumyl; k_{obs} = 0.0245 min^{-1}) > **2a** (^{t}Bu; k_{obs} = 0.011 min^{-1}) > **1a** (^{i}Pr; k_{obs} = 0.0043 min^{-1}) > **8a** (Br; k_{obs} = 0.0016 min^{-1}). Among them, magnesium complex **5a** bearing the most bulky trityl group at the ortho position of the phenolate unit exhibits the highest rate in the polymerization. Complex **1a** with an *o*-isopropyl group shows the lowest activity among those bearing electron-donating substituents but is still more active than complex **8a** with an electron-withdrawing bromo group at the ortho position of the phenolate ring.

When calcium complex **4b** was allowed to polymerize 200 equiv of *rac*-LA in THF at room temperature, a monomer conversion up to 89% could be achieved in 25 min (entry 34), indicating that **4b** was less active than the corresponding magnesium complex **4a** ligated with the same ligand (entry 13). Similar reactivity order was also found for calcium and magnesium complexes with a tripyrazolylborate ligand in the ROP of *rac*-LA.[25] The relatively low reactivity of calcium complex **4b** is probably related with a large radius of the calcium ion, which could not be effectively prevented by the tridentate ligand from aggregation or ligand scrambling.

As shown in Table 4, the solvent has a great impact on the catalytic activity as well. All of the complexes show much higher activity in THF than in toluene. For instance, using complex **1a** as the initiator, a monomer conversion of 90% could be reached within 30 min in THF (entry 1), whereas the yield was just 17% in toluene at room temperature after 420 min. When the reaction temperature was increased to 70 °C, the conversion could be added to 96% in 330 min (entry 3). Therefore, all of the polymerization reactions in toluene were preferably conducted at 70 °C. In toluene, the significantly superior activity of complex **5a** with a trityl group was no longer observed; a more or less similar activity was obtained compared

dx.doi.org/10.1021/ic4012668 | *Inorg. Chem.* 2013, 52, 11821−11835

Table 4. ROP of *rac*-LA Initiated by Complexes 1a−8a and 4b[a]

run	cat.	$[LA]_0/[M]_0/[^iPrOH]_0$	solvent	temp (°C)	time (min)	conv[b] (%)	$M_{n,calcd}$[c] (×10⁴)	M_n[d] (×10⁴)	M_w/M_n[d]	P_r[e]
1	**1a**	200:1:0	THF	25	30	90	2.59	3.24	1.59	0.68
2		200:1:1	THF	25	60	92	2.65	1.93	1.06	0.63
3		200:1:0	Tol	70	330	96	2.77	3.41	1.64	0.48
4		200:1:1	Tol	70	120	90	2.60	2.27	1.51	0.46
5	**2a**	200:1:0	THF	25	30	95	2.74	4.45	1.75	0.70
6		200:1:1	THF	25	60	96	2.77	2.02	1.30	0.69
7		200:1:0	Tol	70	120	90	2.60	3.50	1.48	0.46
8		200:1:1	Tol	70	30	97	2.80	2.57	1.45	0.45
9	**3a**	200:1:0	THF	25	30	93	2.68	3.68	1.60	0.72
10		200:1:1	THF	25	60	95	2.74	2.42	1.40	0.71
11		200:1:0	Tol	70	120	90	2.60	2.80	1.54	0.41
12		200:1:1	Tol	70	30	97	2.80	2.11	1.45	0.40
13	**4a**	200:1:0	THF	25	20	92	2.65	4.27	1.58	0.69
14		200:1:1	THF	25	55	94	2.71	3.06	1.12	0.63
15		200:1:0	Tol	70	120	94	2.71	4.15	1.47	0.46
16		200:1:1	Tol	70	30	96	2.77	3.05	1.33	0.46
17	**5a**	200:1:0	THF	25	1.5	94	2.71	11.9	1.48	0.72
18		200:1:1	THF	25	2	94	2.91	3.04	1.37	0.71
19		200:1:0	THF	−38	2d	92	2.65	21.9	1.44	0.81
20		200:1:0	Tol	70	120	95	2.72	4.73	1.46	0.49
21		200:1:1	Tol	70	30	98	2.82	3.75	1.50	0.49
22	**6a**	200:1:0	THF	25	30	82	2.36	2.98	1.63	0.60
23		200:1:1	THF	25	60	92	2.65	1.42	1.36	0.60
24		200:1:0	Tol	70	240	94	2.71	1.92	1.51	0.50
25		200:1:1	Tol	70	120	90	2.60	2.90	1.21	0.49
26	**7a**	200:1:0	THF	25	30	82	2.36	2.80	1.67	0.73
27		200:1:1	THF	25	480	90	2.59	2.32	1.19	0.68
28		200:1:0	Tol	70	600	92	2.65	2.60	1.46	0.47
29		200:1:1	Tol	70	300	93	2.68	1.89	1.27	0.50
30	**8a**	200:1:0	THF	25	30	86	2.48	2.75	1.43	0.75
31		200:1:1	THF	25	270	84	2.42	1.99	1.20	0.69
32		200:1:0	Tol	70	480	92	2.65	2.70	1.50	0.50
33		200:1:1	Tol	70	300	95	2.74	2.64	1.50	0.49
34	**4b**	200:1:0	THF	25	25	89	2.56	2.89	1.52	0.53
35		200:1:1	THF	25	60	97	2.80	2.69	1.19	0.53
36		200:1:0	Tol	70	60	94	2.71	2.61	1.22	0.43
37		200:1:1	Tol	70	30	94	2.71	2.27	1.23	0.44

[a] $[rac\text{-LA}]_0$ = 1.0 M. [b] Determined by ^{1}H NMR spectroscopy. [c] $M_{n,calcd} = ([LA]_0/[M]_0) \times 144.13 \times$ conv %. [d] Determined by GPC, without correction. [e] P_r is the probability of forming a new r-dyad, determined by homonuclear-decoupled ^{1}H NMR spectroscopy.

to the activities of complexes **2a**−**4a** with a *tert*-butyl or cumyl group (entry 20 vs entries 7, 11, and 15). As we discussed previously, complex **5a** may possess a different coordination environment around the metal center in THF in comparison with the other magnesium complexes, which might account for the significant enhancement of its catalytic activity in THF. Furthermore, consistent with the tendency in THF, magnesium complexes **7a** and **8a** displayed very low activities in toluene with monomer conversions up to 92% achieved in 480 or 600 min.

Generally, the ROPs of *rac*-LA initiated by these alkaline-earth silylamido complexes are not well-controlled, giving moderately distributed polymers (M_w/M_n = 1.12−1.75) because the silylamido group is less nucleophilic than alkoxide and is believed to cause a relatively slow initiation. By using complex **1a** as the initiator to catalyze the ROP of *rac*-LA in THF, the relationship of M_n of the obtained PLA sample versus conversion was plotted (Figure 8), which, however, indicated a linear increase of M_n with conversion. Although the measured M_n values deviate somewhat from the theoretical data and the molecular weight distributions are relatively broad (M_w/M_n = 1.46−1.52), a moderately controlled polymerization process is suggested, where the rate of initiation is not so slow compared to the rate of propagation.

To understand the differences between the initiation by an amide group and an alkoxide group in our system, the *rac*-LA polymerization was carried out with complexes **1a**−**8a** and **4b** in the presence of 2-propanol. Before conducting systematic polymerization studies, the NMR tube reaction of typical complexes **2a**, **2a**·THF, and **5a** with 2-propanol in benzene-d_6 was monitored, respectively. The 1:1 ratio reaction of **2a** or **2a**·THF with 2-propanol generated the same iminophenolato-magnesium alkoxide "[$\mathbf{L}^2$MgO^{i}Pr]", characterized by the proton resonance peaks at 3.29, 2.13, and 1.70 ppm assignable to methoxy, methyl, and *tert*-butyl of the ligand as well as a multiplet at 4.17 ppm and a doublet at 1.20 ppm assignable to the isopropoxyl group (Figure S3 in the SI). In comparison with the original silylamido complex **2a**, the methoxy proton resonance of the formed "[$\mathbf{L}^2$MgO^{i}Pr]" species is significantly upfield-shifted, indicating a dissociated state of this group.

dx.doi.org/10.1021/ic4012668 | *Inorg. Chem.* 2013, 52, 11821−11835

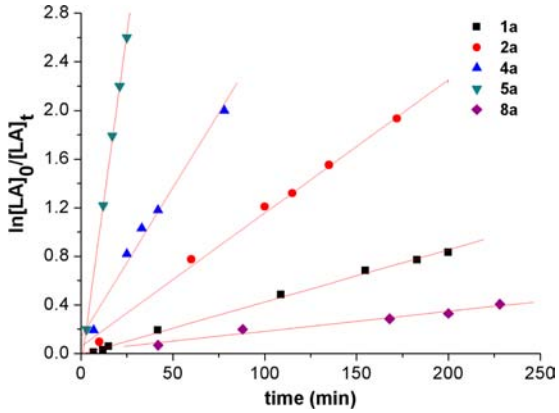

Figure 7. Semilogarithmic plots of LA monomer conversion versus time, $[LA]_0/[Mg]_0$ = 25, $[LA]_0$ = 0.20 M, T = 25 °C, C_6D_6 (0.5 mL): *rac*-LA polymerization using **1a** (black ■), k_{obs} = 0.0043 min^{-1}, R^2 = 0.997, **2a** (red ●), k_{obs} = 0.011 min^{-1}, R^2 = 0.996, **4a** (blue ▲), k_{obs} = 0.0245 min^{-1}, R^2 = 0.983, **5a** (green ▼), k_{obs} = 0.11 min^{-1}, R^2 = 0.999, and **8a** (brown ◆), k_{obs} = 0.0016 min^{-1}, R^2 = 0.967.

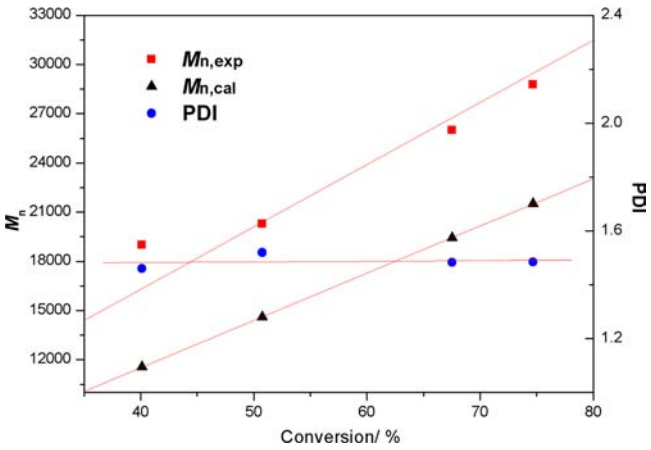

Figure 8. Relationship of M_n and the polydispersity index (PDI) of the PLA sample versus monomer conversion catalyzed by complex **1a** ($[rac\text{-LA}]_0$= 1.0 M, $[rac\text{-LA}]_0$:$[\mathbf{1a}]_0$= 200:1, 25 °C, in THF).

Therefore, it is suggested that the in situ generated magnesium isopropoxide "$[\mathbf{L}^2MgO^iPr]$" should have a dimeric structure, where each magnesium center is four-coordinated, instead of a monomeric structure with a three-coordinated metal center. It is worth noting that, besides the major "$[\mathbf{L}^2MgO^iPr]$" product, there is also a set of signals at 3.19, 2.15, and 1.75 ppm in small amounts in the ^{1}H NMR spectrum, which is in consistent with the resonances of the bisligated magnesium complex $(\mathbf{L}^2)_2Mg$.[26] The percentage of the bisligated complex increased significantly upon standing overnight (in the case of **2a**·THF, from 1:4.5 to 1:1.2), indicative of a relatively fast rearrangement process in solution.

The reaction of **5a** with 2-propanol in a 1:1 ratio generated the expected magnesium isopropoxide "$[\mathbf{L}^5MgO^iPr]$" as the single product (Figures S4 and S5a,b in the SI), suggesting that an increase of the steric hindrance of the ortho substituent could protect efficiently the formed magnesium isopropoxide species from rearrangement or ligand scrambling. The methoxy proton resonance appears at 3.19 ppm, which is 0.21 ppm upfield-shifted from that of complex **5a**. Obviously, the methoxy group in "$[\mathbf{L}^5MgO^iPr]$" is also dissociated from the metal center, and a dimeric structure is therefore suggested. A further addition of 1 equiv more of 2-propanol, however, led to partial decomposition of the formed magnesium isorpopoxide, as indicated by the appearance of free ligand $\mathbf{L}^5\mathbf{H}$.

On the basis of the above studies, the polymerization of *rac*-LA was initiated by the in situ generated magnesium isopropoxide obtained by strictly controlling the molar ratio of the magnesium silylamido complex to 2-propanol at 1:1. As listed in Table 4, the polymerizations of *rac*-LA initiated by complexes **1a**−**8a** and **4b**/2-propanol are well-controlled, affording polymers with relatively narrow molecular weight distributions (M_w/M_n = 1.06−1.40). Meanwhile, the measured molecular weights (M_n) are close to the calculated ones. It is worth noting that, in contrast to our previous results,[7f] the addition of 2-propanol has a different influence on the polymerization conducted in THF or in toluene. In THF, the polymerizations of *rac*-LA initiated by complexes **1a**−**8a** and **4b** in the presence of 2-propanol are unexpectedly slow compared to those without the addition of 2-propanol, while the order in toluene is still consistent with literature reports.[7f,g] For example, using complex **1a** as the initiator, the polymerization proceeded to 90% conversion within 30 min in THF (entry 1), whereas the yield just reached 92% after 60 min (entry 2) in the presence of **1a**/2-propanol under the same polymerization conditions. In toluene, a monomer conversion of 96% could be achieved by **1a** in 330 min; the addition of 2-propanol significantly shortened the polymerization time to 120 min to reach a similar conversion of 90% (entries 3 and 4). It is thus suggested that, although an alkoxide group is superior to an amide group in initiation, a coordinative solvent may bring a complicated effect during the polymerization by either facilitating dissociation of the in situ formed dimeric metal alkoxide species or blocking the coordination site via a competitive coordination to the metal center.

To acquire some insight into the polymerization mechanism of the magnesium complex/2-propanol system, the NMR-scale polymerization was conducted with **2a**·THF in the presence of 1 equiv of 2-propanol with $[rac\text{-LA}]_0$:$[\mathbf{2a}\cdot THF]_0$:$[^iPrOH]_0$ = 20:1:1. The polymerization started instantaneously, and the active oligomer "$\{\mathbf{L}^2Mg[(OCH(CH_3)CO)_nO^iPr]\}$" could be identified unambiguously (Figure S6 in the SI). Meanwhile, a small amount of $(\mathbf{L}^2)_2Mg$ could also be observed in the ^{1}H NMR spectrum, which is inactive for the polymerization. End-group analysis by ^{1}H NMR spectroscopy of the purified oligomer sample showed clearly the existence of both terminal groups of isopropoxy and $HOCH(CH_3)CO-$ according to the resonances at about 1.22 and 5.01 ppm for the former and 1.48 and 4.36 ppm for the latter (Figure S7 in the SI). Electrospray ionization time-of-flight mass spectroscopy (ESI-TOF-MS) further revealed that the oligomers end-capped with $(CH_3)_2CHO-$ and $HOCH(CH_3)CO-$ groups were formed, although there were some transesterification side reactions during the polymerization evidenced by the existence of oligomers with an odd number of lactate units. Accordingly, the polymerization initiated by the magnesium complex/2-propanol system is suggested to proceed via a common "coordination−insertion" mechanism.

Microstructure analyses of PLAs were achieved through inspection of the methine region of homonuclear-decoupled ^{1}H NMR spectra of the resultant polymers. All of the magnesium complexes **1a**−**8a** displayed moderate heterotactic selectivity (P_r = 0.6−0.75) for the ROP of *rac*-LA in THF, whereas atactic or isotactic bias PLAs (P_r = 0.50−0.40) were obtained in toluene. Carpentier and co-workers[27] reported that yttrium

dx.doi.org/10.1021/ic4012668 | Inorg. Chem. 2013, 52, 11821−11835

complexes supported by dianionic alkoxyaminobis(phenolate) ligands showed high heteroselectivity for *rac*-LA polymerization in THF, whereas the propagating species in toluene generated nearly atactic materials. A similar solvent effect was also found by Chisholm and co-workers[28] that magnesium complexes bearing 1,5,9-trimesityldipyrromethene ligands showed much higher stereoselectivity in THF than in a toluene/DCM mixture. On the basis of the results of a computational analysis, Rzepa and co-workers[29] proposed that the high heteroselectivity obtained in the ROP of *rac*-LA by magnesium β-diketiminate complexes in a coordinative solvent might be attributed to a solvent effect, which serves to balance the system entropically.

In comparison with the crucial effect of the solvent, variation of the ligand structure represented by the ortho substituent at the phenoxy moiety has a slight influence on the stereoselectivity. PLAs with nearly the same heteroselectivities were obtained by complexes **1a**−**5a**. Compared to complexes **1a**−**6a**, complexes **7a** and **8a** with a halo substituent displayed a slightly enhanced preference for the heterotactic dyad enchainment in THF (P_r = 0.73 and 0.75, entries 26 and 30; Figure S9 in the SI). At the present stage, we have no reasonable explanation about this point, but it is suggested that a steric effect arising from a certain structure of these two complexes in solution should be responsible for the observed selectivity. Moreover, the only heteroleptic calcium complex **4b** hardly showed selectivity for the ROP of *rac*-LA in both solvents, resulting in atactic to isotactic bias PLAs of high molecular weight, which was in contrast to the moderately heteroselective magnesium complex **4a** with the same ligand (P_r = 0.69, in THF, entry 13). It is implied that the coordination site in calcium complex **4b** is not sufficiently surrounded to impart any stereoselectivity in the ROP event. The P_r values of the obtained polymers also varied slightly upon a change in the polymerization temperature. As listed in Table 4, entry 19, the P_r value of PLA obtained by **5a** in THF increased to 0.81 when the polymerization temperature was decreased to −38 °C (Figure S10 in the SI).

CONCLUSIONS

A series of racemic [ONO]-type iminophenols ($\mathbf{L^1H}$−$\mathbf{L^8H}$) based on the biphenyl skeleton and their magnesium and calcium silylamido complexes were synthesized and structurally characterized. X-ray diffraction studies of typical magnesium complexes revealed that, when a chloro or bromo substituent is introduced to the ortho position of the phenoxide unit, the corresponding magnesium complexes **7a** and **8a** crystallize unexpectedly as dimers, with two metal centers bridging through the oxygen atoms of two phenolato ligands, while the other magnesium complexes are still monomeric in the solid state, possessing a four-coordinate metal core. All of these magnesium and calcium silylamido complexes exhibit good catalytic activity toward *rac*-LA polymerization, and the observed activity increases with an increase in the steric bulkiness of the ortho substituent on the phenoxide unit. Furthermore, calcium complex **4b** is less active than magnesium complex **4a** with the same ligand, and complex **8a** shows a much lower activity among these complexes but the best stereoselectivity for ROP of *rac*-LA in THF at room temperature (P_r = 0.75). Additionally, the most sterically hindered initiator **5a** gains an enhanced heterotactic bias in the polymerization of *rac*-LA in THF at a low temperature of −38 °C, producing heterotactic-enriched PLAs with P_r values up to 0.81.

EXPERIMENTAL SECTION

Materials and Methods. All manipulations were carried out under a dry argon atmosphere using standard Schlenk-line or glovebox techniques. Toluene and *n*-hexane were refluxed over sodium benzophenone ketyl prior to use. Benzene-d_6, chloroform-*d*, and other reagents were carefully dried and stored in a glovebox. $\{Mg[N(SiMe_3)_2]_2\}_2$,[30] $Ca[N(SiMe_3)_2]_2{\cdot}2THF$,[31] 2-hydroxy-3-isopropylbenzaldehyde,[32] 3-*tert*-butyl-2-hydroxy-5-methylbenzaldehyde,[32] 3,5-di-*tert*-butyl-2-hydroxybenzaldehyde,[32] 2-hydroxy-3,5-dicumylbenzaldehyde,[32] 5-*tert*-butyl-2-hydroxy-3-tritylbenzaldehyde,[33] 5-*tert*-butyl-3-chloro-2-hydroxybenzaldehyde,[34] and 5-*tert*-butyl-3-bromo-2-hydroxybenzaldehyde,[35] were synthesized according to literature methods. *rac*-LA (Aldrich) was recrystallized with dry toluene and then sublimed twice under vacuum at 80 °C. 2-Propanol was dried over calcium hydride prior to distillation. All other chemicals were commercially available and used after appropriate purification. Glassware and vials used in the polymerization were dried in an oven at 120 °C overnight and exposed to a vacuum−argon cycle three times.

Measurements. NMR spectra were recorded on a Bruker AVANCE-400 spectrometer at 25 °C (^{1}H, 400 MHz; ^{13}C, 100 MHz) unless otherwise stated. Chemical shifts for ^{1}H and ^{13}C NMR spectra were referenced internally using the residual solvent resonances and reported relative to tetramethylsilane. Elemental analyses were performed on an EA-1106 instrument. Spectroscopic analyses of polymers were performed in $CDCl_3$. Gel permeation chromatography (GPC) analyses were carried out on an Agilent instrument (L1200 pump, Optilab Rex injector) in THF at 25 °C at a flow rate of 1 mL·min^{-1}. Calibration standards were commercially available narrowly distributed linear polystyrene samples that cover a broad range of molar masses ($10^3 < M_n < 2 \times 10^6$ g·mol^{-1}). The M_n values were reported without correction.

Syntheses. *2-[(2′-Methoxybiphenyl-2-ylimino)methyl]-6-isopropylphenol ($\mathbf{L^1H}$).* 2-Hydroxy-3-isopropylbenzaldehyde (0.821 g, 5.00 mmol) was mixed with 2-methoxy-2′-amidobiphenyl (0.996 g, 5.00 mmol) in ethanol (50 mL). The mixture was refluxed at 80 °C and stirred for 5 h at this temperature. After cooling to room temperature, the solution was concentrated to about 20 mL and kept at −20 °C. Yellow crystalline solids could be obtained in 80% yield (1.209 g). ^{1}H NMR ($CDCl_3$, 400 MHz, 298 K): δ 13.05 (s, 1H, O*H*), 8.49 (s, 1H, NC*H*Ar), 7.38 (m, 2H, Ar*H*), 7.32 (m, 2H, Ar*H*), 7.22 (t, 2H, J = 7.2 Hz, Ar*H*), 7.17 (d, 1H, J = 7.8 Hz, Ar*H*), 7.13 (d, 1H, J = 7.5 Hz, Ar*H*), 6.99 (t, 1H, J = 7.5 Hz, Ar*H*), 6.91 (d, 1H, J = 8.0 Hz, Ar*H*), 6.82 (t, 1H, J = 7.6 Hz, Ar*H*), 3.68 (s, 3H, C*H*$_3$OAr), 3.30 (sept, 1H, J = 6.9 Hz, ArC*H*(CH$_3$)$_2$), 1.19 (d, 6H, J = 6.9 Hz, CH(C*H*$_3$)$_2$). ^{13}C{^{1}H} NMR ($CDCl_3$, 100 MHz): δ 162.7, 158.6, 156.4, 147.5, 136.3, 133.7, 131.3, 131.1, 129.6, 129.4, 129.0, 128.5, 128.4, 126.4, 120.4, 118.6, 118.28, 118.27, 110.6 (NCHAr and all ArC), 55.2 (*C*H$_3$OAr), 26.4 (ArCH(*C*H$_3$)$_2$), 22.2 (ArCH(*C*H$_3$)$_2$). HRMS. Calcd for $C_{23}H_{23}NO_2$: 345.1729. Found: 345.1726.

2-[(2′-Methoxybiphenyl-2-ylimino)methyl]-4-methyl-6-tert-butylphenol ($\mathbf{L^2H}$). The procedure was the same as that of $\mathbf{L^1H}$, except that 3-*tert*-butyl-2-hydroxy-5-methylbenzaldehyde (0.961 g, 5.00 mmol) and 2-methoxy-2′-amidobiphenyl (0.996 g, 5.00 mmol) were used to afford ligand $\mathbf{L^2H}$ as yellow crystalline solids in 80% yield (1.494 g). ^{1}H NMR ($CDCl_3$, 400 MHz, 298 K): δ 13.35 (s, 1H, O*H*), 8.47 (s, 1H, NC*H*Ar), 7.41 (m, 2H, Ar*H*), 7.34 (t, 2H, J = 7.5 Hz, Ar*H*), 7.22 (m, 2H, Ar*H*), 7.12 (s, 1H, Ar*H*), 7.00 (t, 1H, J = 7.4 Hz, Ar*H*), 6.96 (m, 2H, Ar*H*), 3.73 (s, 3H, C*H*$_3$OAr), 2.28 (s, 3H, C*H*$_3$Ar), 1.37 (s, 9H, C(C*H*$_3$)$_3$). ^{13}C{^{1}H} NMR ($CDCl_3$, 100 MHz, 298 K): δ 162.7, 158.3, 156.5, 147.3, 137.2, 133.9, 131.3, 131.1, 131.0, 130.1, 129.0, 128.5, 128.4, 126.5, 126.4, 120.3, 118.8, 118.1, 110.5 (NCHAr and all ArC), 55.2 (*C*H$_3$OAr), 34.7 (*C*(CH$_3$)$_3$), 29.2 (C(*C*H$_3$)$_3$), 20.6 (*C*H$_3$Ar). HRMS. Calcd for $C_{25}H_{27}NO_2$: 373.2042. Found: 373.2041.

2-[(2′-Methoxybiphenyl-2-ylimino)methyl]-4,6-di-tert-butylphenol ($\mathbf{L^3H}$). The procedure was the same as that of $\mathbf{L^1H}$, except that 3,5-

di-*tert*-butyl-2-hydroxybenzaldehyde (1.172 g, 5.000 mmol) and 2-methoxy-2′-amidobiphenyl (0.996 g, 5.00 mmol) were used to afford ligand **L^{3}H** as yellow crystalline solids in 82% yield (1.704 g). ^{1}H NMR ($CDCl_3$, 400 MHz, 298 K): δ 13.40 (s, 1H, O*H*), 8.53 (s, 1H, NC*H*Ar), 7.43−7.38 (m, 3H, Ar*H*), 7.34 (m, 2H, Ar*H*), 7.21 (m, 2H, Ar*H*), 7.15 (d, 1H, J = 2.3 Hz, Ar*H*), 6.99 (t, 1H, J = 7.4 Hz, Ar*H*), 6.95 (d, 1H, J = 8.3 Hz, Ar*H*), 3.77 (s, 3H, C*H*$_3$OAr), 1.39 (s, 9H, C(C*H*$_3$)$_3$), 1.31 (s, 9H, C(C*H*$_3$)$_3$). ^{13}C{^{1}H} NMR ($CDCl_3$, 100 MHz, 298 K): δ 163.1, 158.2, 156.5, 147.4, 140.0, 136.7, 134.1, 131.3, 131.0, 128.9, 128.50, 128.46, 127.6, 126.42, 126.37, 120.3, 118.3, 118.0, 110.5, (NCHAr and all Ar*C*), 55.2 (*C*H$_3$OAr), 35.0 (*C*(CH$_3$)$_3$), 34.1 (*C*(CH$_3$)$_3$), 31.4 (C(*C*H$_3$)$_3$), 29.3 (C(*C*H$_3$)$_3$). HRMS. Calcd for $C_{28}H_{33}NO_2$: 415.2511. Found: 415.2509.

*2-[(2′-Methoxybiphenyl-2-ylimino)methyl]-4,6-dicumylphenol (**L^{4}H**).* The procedure was the same as that of **L^{1}H**, except that 2-hydroxy-3,5-dicumylbenzaldehyde (1.792 g, 5.000 mmol) and 2-methoxy-2′-amidobiphenyl (0.996 g, 5.00 mmol) were used to afford ligand **L^{4}H** as an orange viscous oil in 75% yield (2.024 g). ^{1}H NMR ($CDCl_3$, 400 MHz, 298 K): δ 13.09 (s, 1H, O*H*), 8.39 (s, 1H, NC*H*Ar), 7.36−7.28 (m, 5H, Ar*H*), 7.25 (m, 3H, Ar*H*), 7.24−7.18 (m, 4H, Ar*H*), 7.13 (m, 4H, Ar*H*), 7.04 (m, 2H, Ar*H*), 6.88 (t, 1H, J = 7.4 Hz, Ar*H*), 6.61 (d, 1H, J = 8.3 Hz, Ar*H*), 3.35 (s, 3H, C*H*$_3$OAr), 1.69 (s, 6H, C(C*H*$_3$)$_2$Ph), 1.58 (s, 6H, C(C*H*$_3$)$_2$Ph). ^{13}C{^{1}H} NMR ($CDCl_3$, 100 MHz, 298 K): δ 162.2, 157.7, 156.1, 150.7, 146.9, 139.4, 136.4, 134.2, 131.1, 130.8, 129.2, 128.7, 128.4, 128.2, 128.0, 127.5, 126.7, 126.5, 125.7, 125.6, 124.7, 120.0, 118.3, 117.6, 110.5 (NCHAr and all Ar*C*), 54.8 (*C*H$_3$OAr), 42.4 (*C*(CH$_3$)$_2$Ph), 41.9 (*C*(CH$_3$)$_2$Ph), 30.9 (C(*C*H$_3$)$_2$Ph), 29.0 (C(*C*H$_3$)$_2$Ph). HRMS. Calcd for $C_{38}H_{37}NO_2$: 539.2824. Found: 539.2827.

*2-[(2′-Methoxybiphenyl-2-ylimino)methyl]-4-tert-butyl-6-tritylphenol (**L^{5}H**).* The procedure was the same as that of **L^{1}H**, except that 5-*tert*-butyl-2-hydroxy-3-tritylbenzaldehyde (2.101 g, 5.000 mmol) and 2-methoxy-2′-amidobiphenyl (0.996 g, 5.00 mmol) were used to afford ligand **L^{5}H** as yellow crystalline solids in 72% yield (2.165 g). ^{1}H NMR ($CDCl_3$, 400 MHz, 298 K): δ 13.10 (s, 1H, O*H*), 8.43 (s, 1H, NC*H*Ar), 7.38 (m, 2H, Ar*H*), 7.29 (m, 2H, Ar*H*), 7.18−7.10 (m, 18H, Ar*H*), 7.04 (dd, 1H, J = 7.3 and 1.2 Hz, Ar*H*), 6.88 (t, 1H, J = 7.3 Hz, Ar*H*), 6.56 (d, 1H, J = 8.0 Hz, Ar*H*), 3.24 (s, 3H, C*H*$_3$OAr), 1.70 (s, 9H, C(C*H*$_3$)$_3$). ^{13}C{^{1}H} NMR ($CDCl_3$, 100 MHz, 298 K): δ 162.6, 158.0, 155.9, 147.2, 145.5, 139.7, 134.1, 134.0, 132.2, 131.1, 131.0, 130.84, 130.78, 129.0, 128.8, 128.4, 128.2, 128.0, 127.3, 127.0, 126.4, 125.3, 120.0, 118.5, 118.2, 110.7 (NCHAr and all Ar*C*), 63.4 (Ar*C*Ph$_3$), 54.8 (*C*H$_3$OAr), 34.0 (*C*(CH$_3$)$_3$), 31.3 (C(*C*H$_3$)$_3$). HRMS. Calcd for $C_{43}H_{39}NO_2$: 601.2981. Found: 601.2980.

*2-[(2′-Methoxybiphenyl-2-ylimino)methyl]-4-tert-butyl-6-(piperidin-1-ylmethyl)phenol (**L^{6}H**).* The procedure was the same as that of **L^{1}H**, except that 5-*tert*-butyl-2-hydroxy-3-[(piperidin-1-yl)methyl]-benzaldehyde (1.377 g, 5.000 mmol) and 2-methoxy-2′-amidobiphenyl (0.996 g, 5.00 mmol) were used to afford ligand **L^{6}H** as yellow crystalline solids in 86% yield (1.963 g). ^{1}H NMR ($CDCl_3$, 400 MHz, 298 K): δ 8.57 (s, 1H, NC*H*Ar), 7.40 (m, 3H, Ar*H*), 7.32 (m, 2H, Ar*H*), 7.26 (s, 1H, Ar*H*), 7.23 (dd, 1H, J = 7.2 and 1.6 Hz, Ar*H*), 7.19 (d, 1H, J = 8.0 Hz, Ar*H*), 7.00 (t, 1H, J = 7.4 Hz, Ar*H*), 6.92 (d, 1H, J = 8.2 Hz, Ar*H*), 3.72 (s, 3H, C*H*$_3$OAr), 3.57 (s, 2H, NC*H*$_2$Ar), 2.44 (br, 4H, NC*H*$_2$CH$_2$), 1.60 (m, 4H, NCH$_2$C*H*$_2$), 1.44 (m, 2H, CH$_2$C*H*$_2$CH$_2$), 1.30 (s, 9H, C(C*H*$_3$)$_3$). ^{13}C{^{1}H} NMR ($CDCl_3$, 100 MHz, 298 K): δ 162.0, 157.2, 156.5, 148.2, 140.6, 133.7, 131.3, 131.2, 131.0, 128.8, 128.6, 128.4, 126.5, 126.1, 124.7, 120.3, 118.8, 118.2, 110.7 (NCHAr and all Ar*C*), 57.1 (NCH$_2$Ar), 55.3 (CH$_3$OAr), 54.2 (NCH$_2$CH$_2$), 33.9 (*C*(CH$_3$)$_3$), 31.4 (C(*C*H$_3$)$_3$), 26.0 (NCH$_2$CH$_2$), 24.3 (CH$_2$CH$_2$CH$_2$). HRMS. Calcd for $C_{30}H_{36}N_2O_2$: 456.2777. Found: 456.2774.

*2-[(2′-Methoxybiphenyl-2-ylimino)methyl]-4-tert-butyl-6-chlorophenol (**L^{7}H**).* The procedure was the same as that of **L^{1}H**, except that 5-*tert*-butyl-3-chloro-2-hydroxybenzaldehyde (1.063 g, 5.000 mmol) and 2-methoxy-2′-amidobiphenyl (0.996 g, 5.00 mmol) were used to afford ligand **L^{7}H** as orange crystalline solids in 86% yield (1.694 g). ^{1}H NMR ($CDCl_3$, 400 MHz, 298 K): δ 13.17 (s, 1H, O*H*), 8.51 (s, 1H, NC*H*Ar), 7.43 (m, 2H, Ar*H*), 7.36 (m, 3H, Ar*H*), 7.21 (m, 3H, Ar*H*), 7.01 (t, 1H, J = 7.4 Hz, Ar*H*), 6.95 (d, 1H, J = 8.3 Hz, Ar*H*), 3.73 (s, 3H, C*H*$_3$OAr), 1.30 (s, 9H, C(C*H*$_3$)$_3$). ^{13}C{^{1}H} NMR ($CDCl_3$, 100 MHz, 298 K): δ 162.0, 156.4, 155.5, 147.0, 142.0, 133.9, 131.3, 131.2, 130.5, 129.3, 128.5, 128.1, 127.0, 126.8, 121.0, 120.6, 119.5, 118.3, 110.9, (NCHAr and all Ar*C*), 55.4 (CH$_3$OAr), 34.1 (*C*(CH$_3$)$_3$), 31.2 (C(*C*H$_3$)$_3$). HRMS. Calcd for $C_{24}H_{24}ClNO_2$: 393.1496. Found: 393.1488.

*2-[(2′-Methoxybiphenyl-2-ylimino)methyl]-4-tert-butyl-6-bromophenol (**L^{8}H**).* The procedure was same as that of **L^{1}H**, except that 5-*tert*-butyl-3-bromo-2-hydroxybenzaldehyde (1.286 g, 5.000 mmol) and 2-methoxy-2′-amidobiphenyl (0.996 g, 5.00 mmol) were used to afford ligand **L^{8}H** as orange crystalline solids in 89% yield (1.951 g). ^{1}H NMR ($CDCl_3$, 400 MHz, 298 K): δ 13.30 (s, 1H, O*H*), 8.47 (s, 1H, NC*H*Ar), 7.59 (d, 1H, J = 2.3 Hz, Ar*H*), 7.45−7.32 (m, 4H, Ar*H*), 7.25 (d, 1H, J = 2.3 Hz, Ar*H*), 7.21 (m, 2H, Ar*H*), 7.01 (t, 1H, J = 7.4 Hz, Ar*H*), 6.95 (d, 1H, J = 8.3 Hz, Ar*H*), 3.73 (s, 3H, C*H*$_3$OAr), 1.30 (s, 9H, C(C*H*$_3$)$_3$). ^{13}C{^{1}H} NMR ($CDCl_3$, 100 MHz, 298 K): δ 162.0, 156.3, 155.5, 147.0, 142.5, 133.9, 133.5, 131.3, 131.2, 129.3, 128.5, 128.1, 127.9, 126.8, 120.6, 119.4, 118.4, 110.9, 110.5 (NCHAr and all Ar*C*), 55.3 (*C*H$_3$OAr), 34.1 (*C*(CH$_3$)$_3$), 31.3 (C(*C*H$_3$)$_3$). HRMS. Calcd for $C_{24}H_{25}BrNO_2$ [M + H]: 438.1069. Found: 438.1063.

*[(**L^1**)MgN(SiMe$_3$)$_2$] (**1a**).* In a glovebox, the ligand **L^{1}H** (0.345 g, 1.00 mmol) was added slowly to a solution of {Mg[N(SiMe$_3$)$_2$]$_2$}$_2$ (0.345 g, 0.500 mmol) in toluene (20 mL). The reaction solution was stirred at room temperature for 24 h. All of the volatiles were removed under vacuum. The resultant yellow solids were recrystallized with a mixture of toluene and *n*-hexane at −38 °C to afford yellow crystalline solids in 53% yield (0.280 g). ^{1}H NMR (C_6D_6, 400 MHz, 298 K): δ 7.64 (s, 1H, NC*H*Ar), 7.16 (d, 1H, J = 7.2 Hz, Ar*H*), 7.09 (m, 1H, Ar*H*), 7.01 (m, 2H, Ar*H*), 6.86 (d, 1H, J = 7.7 Hz, Ar*H*), 6.78 (d, 2H, J = 7.3 Hz, Ar*H*), 6.67 (m, 3H, Ar*H*), 6.46 (t, 1H, J = 7.5 Hz, Ar*H*), 3.82 (sept, 1H, J = 6.9 Hz, C*H*(CH$_3$)$_2$), 3.61 (s, 3H, C*H*$_3$OAr), 1.37 (d, 3H, J = 6.9 Hz, CH(C*H*$_3$)$_2$), 1.25 (d, 3H, J = 6.9 Hz, CH(C*H*$_3$)$_2$), 0.39 (s, 18H, N(Si(C*H*$_3$)$_3$)$_2$). ^{13}C{^{1}H} NMR (C_6D_6, 100 MHz, 298 K): δ 173.6, 169.3, 153.4, 150.1, 141.7, 133.6, 132.4, 132.3, 132.1, 131.5, 130.2, 130.24, 130.04, 127.4, 126.8, 124.0, 121.7, 119.2, 114.4 (NCHAr and all Ar*C*), 66.1 (*C*H$_3$OAr), 27.2 (CH(*C*H$_3$)$_2$), 23.0 (CH(*C*H$_3$)$_2$), 22.3 (CH(*C*H$_3$)$_2$), 5.7 (N(Si(*C*H$_3$)$_3$)$_2$). Anal. Calcd for $C_{29}H_{40}MgN_2O_2Si_2$: C, 65.83; H, 7.62; N, 5.29. Found: C, 65.73; H, 7.65; N, 5.22.

*[(**L^2**)MgN(SiMe$_3$)$_2$] (**2a**).* Following a procedure similar to that described for **1a**, **L^{2}H** (0.373 g, 1.00 mmol) was treated with {Mg[N(SiMe$_3$)$_2$]$_2$}$_2$ (0.345 g, 0.500 mmol) in toluene (20 mL) at room temperature to give yellow solids after workup. Yellow crystals could be obtained after recrystallization from a mixture of toluene and *n*-hexane at −38 °C in 52% yield (0.290 g). ^{1}H NMR (C_6D_6, 400 MHz, 298 K): δ 7.60 (s, 1H, NC*H*Ar), 7.20 (s, 1H, Ar*H*), 7.15 (s, 2H, Ar*H*), 7.12 (m, 2H, Ar*H*), 7.01 (m, 5H, Ar*H*), 6.82 (d, 1H, J = 7.3 Hz, Ar*H*), 6.79 (d, 1H, J = 7.3 Hz, Ar*H*), 6.71 (m, 2H, Ar*H*), 6.37 (s, 1H, Ar*H*), 3.57 (s, 3H, C*H*$_3$OAr), 2.10 (s, 3H, C*H*$_3$Tol), 2.06 (s, 3H, C*H*$_3$Ar), 1.64 (s, 9H, C(C*H*$_3$)$_3$), 0.40 (s, 18H, N(Si(C*H*$_3$)$_3$)$_2$). ^{13}C{^{1}H} NMR (C_6D_6, 100 MHz, 298 K): δ 173.6, 169.0, 153.5, 150.4, 141.8, 134.7, 133.7, 132.6, 132.2, 131.6, 130.2, 130.0, 129.3, 128.5, 127.9, 127.5, 126.7, 125.6, 124.0, 122.0, 121.7, 120.9, 119.8 (NCHAr and all Ar*C*), 66.0 (*C*H$_3$OAr), 35.4 (*C*(CH$_3$)$_3$), 29.7 (C(*C*H$_3$)$_3$), 21.4 (*C*H$_3$Tol), 20.5 (*C*H$_3$Ar), 5.7 (N(Si(*C*H$_3$)$_3$)$_2$). Anal. Calcd for $C_{31}H_{44}MgN_2O_2Si_2{\cdot}C_7H_8$: C, 70.29; H, 8.07; N, 4.31. Found: C, 70.48; H, 8.07; N, 4.15.

*[(**L^2**)MgN(SiMe$_3$)$_2$·THF] (**2a**·THF).* Complex **2a**·THF was obtained as yellow crystals by recrystallizing complex **2a** in a THF/*n*-hexane mixture at −38 °C. ^{1}H NMR (C_6D_6, 400 MHz, 298 K): δ 7.86 (s, 1H, NC*H*Ar), 7.24 (d, 1H, J = 2.2 Hz, Ar*H*), 7.18 (m, 1H, Ar*H*), 7.13−7.07 (m, 2H, Ar*H*), 7.03 (m, 2H, Ar*H*), 6.83 (t, 1H, J = 7.5 Hz, Ar*H*), 6.73 (t, 1H, J = 7.5 Hz, Ar*H*), 6.62 (d, 1H, J = 8.0 Hz, Ar*H*), 6.46 (s, 1H, Ar*H*), 3.49 (br, 4H, THF), 3.38 (s, 3H, C*H*$_3$OAr), 2.09 (s, 3H, C*H*$_3$Ar), 1.62 (s, 9H, C(C*H*$_3$)$_3$), 1.31 (br, 4H, THF), 0.37 (s, 18H, N(Si(C*H*$_3$)$_3$)$_2$). ^{13}C{^{1}H} NMR (C_6D_6, 100 MHz, 298 K): δ 174.7, 168.8, 155.3, 150.7, 141.5, 134.5, 134.0, 132.1, 132.0, 131.2, 130.8, 129.7, 129.3, 126.4, 124.6, 123.8, 121.9, 119.9, 115.9 (NCHAr and all Ar*C*), 68.4 (THF), 60.0 (*C*H$_3$OAr), 35.4 (*C*(CH$_3$)$_3$), 29.8 (C(*C*H$_3$)$_3$), 25.4 (THF), 20.6 (*C*H$_3$Ar), 5.9 (N(Si(*C*H$_3$)$_3$)$_2$). Anal. Calcd for

dx.doi.org/10.1021/ic4012668 | *Inorg. Chem.* 2013, 52, 11821−11835

$C_{31}H_{44}MgN_2O_2Si_2{\cdot}C_4H_8O$: C, 66.91; H, 8.18; N, 4.46. Found: C, 66.42; H, 8.40; N, 4.21.

*[(L³)MgN(SiMe₃)₂] (**3a**).* Following a procedure similar to that described for **1a**, L^3H (0.415 g, 1.00 mmol) was treated with $\{Mg[N(SiMe_3)_2]_2\}_2$ (0.345 g, 0.500 mmol) in toluene (20 mL) at room temperature to give yellow solids after workup. Recrystallization with a mixture of toluene and *n*-hexane at −38 °C afforded yellow crystalline solids in 55% yield (0.329 g). ^{1}H NMR (C_6D_6, 400 MHz, 298 K): δ 7.67 (s, 1H, NC*H*Ar), 7.57 (s, 1H, Ar*H*), 7.11 (t, 1H, J = 8.0 Hz, Ar*H*), 7.02 (m, 2H, Ar*H*), 6.92 (d, 1H, J = 7.6 Hz, Ar*H*), 6.83 (m, 2H, Ar*H*), 6.70 (m, 3H, Ar*H*), 3.59 (s, 3H, CH_3OAr), 1.67 (s, 9H, C(CH_3)$_3$), 1.22 (s, 9H, C(CH_3)$_3$), 0.39 (s, 18H, N(Si(CH_3)$_3$)$_2$). ^{13}C{^{1}H} NMR (C_6D_6, 100 MHz, 298 K): δ 174.0, 169.0, 153.5, 150.4, 141.5, 135.5, 132.6, 132.2, 131.6, 131.2, 130.2, 130.0, 129.97, 129.94, 127.6, 126.7, 124.1, 121.7, 119.3 (NCHAr and all Ar*C*), 66.0 (CH_3OAr), 35.8 (*C*(CH_3)$_3$), 33.9 (C(CH_3)$_3$), 31.5 (C(*C*H_3)$_3$), 29.7 (C(CH_3)$_3$), 5.8 (N(Si(*C*H_3)$_3$)$_2$). Anal. Calcd for $C_{34}H_{50}MgN_2O_2Si_2$: C, 68.15; H, 8.41; N, 4.67. Found: C, 68.14; H, 8.51; N, 4.54.

*[(L⁴)MgN(SiMe₃)₂] (**4a**).* Following a procedure similar to that described for **1a**, L^4H (0.540 g, 1.00 mmol) was treated with $\{Mg[N(SiMe_3)_2]_2\}_2$ (0.345 g, 0.500 mmol) in toluene (20 mL) at room temperature to give yellow solids after workup. Recrystallization with a mixture of toluene and *n*-hexane at −38 °C afforded yellow crystalline solids in 56% yield (0.405 g). ^{1}H NMR (C_6D_6, 400 MHz, 298 K): δ 7.64 (s, 1H, NC*H*Ar), 7.41 (d, 1H, J = 2.6 Hz, Ar*H*), 7.26 (d, 2H, J = 7.0 Hz, Ar*H*), 7.18 (m, 4H, Ar*H*), 7.09 (m, 4H, Ar*H*), 7.00 (m, 3H, Ar*H*), 6.91 (d, 1H, J = 7.8 Hz, Ar*H*), 6.77 (m, 3H, Ar*H*), 6.66 (t, 1H, J = 7.0 Hz, Ar*H*), 6.53 (d, 1H, J = 8.0 Hz, Ar*H*), 3.45 (s, 3H, CH_3OAr), 2.00 (br s, 3H, C(CH_3)$_2$Ph), 1.54 (s, 9H, C(CH_3)$_2$Ph), 0.26 (s, 18H, N(Si(CH_3)$_3$)$_2$). ^{13}C{^{1}H} NMR (C_6D_6, 100 MHz, 298 K): δ 173.3, 168.4, 153.3, 151.9, 151.1, 150.3, 141.4, 135.2, 133.8, 132.3, 131.9, 131.7, 131.6, 130.0, 129.9, 129.8, 127.5, 127.1, 126.7, 126.2, 125.8, 124.5, 124.0, 122.1, 119.2 (NCHAr and all Ar*C*), 65.8 (CH_3OAr), 43.0 (*C*(CH_3)$_2$Ph), 42.4 (*C*(CH_3)$_2$Ph), 31.9 (C-(CH_3)$_2$Ph), 31.0 (C(*C*H_3)$_2$Ph), 5.8 (N(Si(CH_3)$_3$)$_2$). Anal. Calcd for $C_{44}H_{54}MgN_2O_2Si_2$: C, 73.05; H, 7.52; N, 3.87. Found: C, 72.52; H, 7.46; N, 3.62.

*[(L⁵)MgN(SiMe₃)₂] (**5a**).* Following a procedure similar to that described for **1a**, L^5H (0.602 g, 1.00 mmol) was treated with $\{Mg[N(SiMe_3)_2]_2\}_2$ (0.345 g, 0.500 mmol) in toluene (20 mL) at room temperature to give yellow solids after workup. Recrystallization with a mixture of toluene and *n*-hexane at −38 °C afforded yellow crystalline solids in 50% yield (0.395 g). ^{1}H NMR (C_6D_6, 400 MHz, 298 K): δ 7.63 (s, 1H, NC*H*Ar), 7.59 (d, 1H, J = 2.7 Hz, Ar*H*), 7.49 (m, 6H, Ar*H*), 7.17 (m, 8H, Ar*H*), 7.09 (m, 4H, Ar*H*), 7.01 (m, 2H, Ar*H*), 6.80 (d, 1H, J = 7.6 Hz, Ar*H*), 6.74 (d, 1H, J = 2.6 Hz, Ar*H*), 6.69 (t, 1H, J = 7.6 Hz, Ar*H*), 6.60 (d, 1H, J = 7.8 Hz, Ar*H*), 3.40 (s, 3H, CH_3OAr), 1.05 (s, 3H, C(CH_3)$_3$), 0.15 (s, 18H, N(Si(CH_3)$_3$)$_2$). ^{13}C{^{1}H} NMR (C_6D_6, 100 MHz, 298 K): δ 173.6, 168.0, 153.5, 150.6, 139.7, 136.7, 135.1, 132.3, 131.8, 131.6, 131.2, 129.8, 129.6, 127.5, 126.8, 125.5, 123.9, 122.2, 119.6 (NCHAr and all ArC; ArC signals could not be fully detected because of the poor solubility of **5a** in C_6D_6), 65.9 (CH_3OAr), 64.4 ($ArCPh_3$), 33.8 (*C*(CH_3)$_3$), 31.2 (C(CH_3)$_3$), 5.8 (N(Si(CH_3)$_3$)$_2$). Anal. Calcd for $C_{49}H_{56}MgN_2O_2Si_2$: C, 74.93; H, 7.19; N, 3.57. Found: C, 74.68; H, 7.19; N, 3.34.

*[(L⁶)MgN(SiMe₃)₂] (**6a**).* Following a procedure similar to that described for **1a**, L^6H (0.456 g, 1.00 mmol) was treated with $\{Mg[N(SiMe_3)_2]_2\}_2$ (0.345 g, 0.500 mmol) in toluene (20 mL) at room temperature to give yellow solids after workup. Recrystallization with a mixture of toluene and *n*-hexane at room temperature afforded yellow crystals in 53% yield (0.339 g). ^{1}H NMR (C_6D_6, 400 MHz, 298 K): δ 7.84 (d, 1H, J = 2.6 Hz, Ar*H*), 7.68 (s, 1H, NC*H*Ar), 7.12 (m, 1H, Ar*H*), 7.05 (m, 2H, Ar*H*), 6.90 (d, 1H, J = 7.6 Hz, Ar*H*), 6.85−6.80 (br, 2H, Ar*H*), 6.72 (m, 3H, Ar*H*), 3.87 (br s, 1H, NCH_2Ar), 3.81 (br s, 1H, NCH_2Ar), 3.65 (s, 3H, CH_3OAr), 2.50 (br, 4H, NCH_2CH_2−), 1.57 (br, 4H, NCH_2CH_2−), 1.38 (br, 2H, CH_2CH_2CH_2), 1.23 (s, 9H, C(CH_3)$_3$), 0.39 (s, 18H, N(Si(CH_3)$_3$)$_2$). ^{13}C{^{1}H} NMR (C_6D_6, 100 MHz, 298 K): δ 173.6, 168.5, 153.5, 150.3, 136.1, 134.7, 132.5, 132.3, 131.72, 131.68, 130.2, 130.0, 129.9, 129.6, 127.4, 126.8, 124.2, 121.8, 118.3 (NCHAr and all Ar*C*), 66.1 (CH_3OAr), 57.7 (NCH_2Ar), 55.1 (NCH_2CH_2), 33.8 (*C*(CH_3)$_3$), 31.5 (C(CH_3)$_3$), 26.8 (NCH_2CH_2), 25.1 (CH_2CH_2CH_2), 5.8 (N(Si(CH_3)$_3$)$_2$). Anal. Calcd for $C_{36}H_{53}MgN_3O_2Si_2$: C, 67.53; H, 8.34; N, 6.56. Found: C, 67.98; H, 8.06; N, 6.67.

*[(L⁷)MgN(SiMe₃)₂]₂ (**7a**).* Following a procedure similar to that described for **1a**, L^7H (0.394 g, 1.00 mmol) was treated with $\{Mg[N(SiMe_3)_2]_2\}_2$ (0.345 g, 0.500 mmol) in toluene (20 mL) at room temperature to give yellow solids after workup. Recrystallization with a mixture of toluene and *n*-hexane at room temperature afforded yellow crystals in 52% yield (0.299 g). ^{1}H NMR (C_6D_6, 400 MHz, 298 K): δ 7.54 (s, 1H, NC*H*Ar), 7.52 (d, 1H, J = 2.6 Hz, Ar*H*), 7.09 (m, 1H, Ar*H*), 7.02 (m, 2H, Ar*H*), 6.82 (m, 2H, Ar*H*), 6.73 (m, 1H, Ar*H*), 6.71−6.67 (m, 2H, Ar*H*), 6.58 (d, 1H, J = 2.6 Hz, Ar*H*), 3.61 (s, 3H, CH_3OAr), 1.01 (s, 9H, ArC(CH_3)$_3$), 0.41 (s, 18H, N(Si(CH_3)$_3$)$_2$). ^{13}C{^{1}H} NMR (C_6D_6, 100 MHz, 298 K): δ 173.3, 164.1, 153.2, 149.7, 136.6, 133.9, 132.2, 132.0, 131.5, 130.5, 130.2, 129.9, 129.7, 127.4, 127.1, 123.8, 121.9, 121.6, 119.4 (NCHAr and all Ar*C*), 66.1 (*C*H_3OAr), 33.6 (C(CH_3)$_3$), 31.2 (C(CH_3)$_3$), 5.8 (N(Si(CH_3)$_3$)$_2$). Anal. Calcd for $C_{60}H_{82}Cl_2Mg_2N_4O_4Si_4$: C, 62.38; H, 7.15; N, 4.85. Found: C, 61.75; H, 7.11; N, 4.82.

*[(L⁸)MgN(SiMe₃)₂] (**8a**).* Following a procedure similar to that described for **1a**, L^8H (0.438 g, 1.00 mmol) was treated with $\{Mg[N(SiMe_3)_2]_2\}_2$ (0.345 g, 0.500 mmol) in toluene (20 mL) at room temperature to give yellow solids after workup. Recrystallization with a mixture of toluene and *n*-hexane at room temperature afforded yellow crystals in 52% yield (0.322 g). ^{1}H NMR (C_6D_6, 400 MHz, 298 K): δ 7.73 (d, 1H, J = 2.5 Hz, Ar*H*), 7.52 (s, 1H, NC*H*Ar), 7.11−7.07 (m, 1H, Ar*H*), 7.02 (m, 2H, Ar*H*), 6.82 (m, 2H, Ar*H*), 6.76 (dd, 1H, J = 7.7 and 1.4 Hz, Ar*H*), 6.72−6.65 (br m, 2H, Ar*H*), 6.62 (d, 1H, J = 2.5 Hz, Ar*H*), 3.62 (s, 3H, CH_3OAr), 1.00 (s, 9H, C(CH_3)$_3$), 0.41 (s, 18H, N(Si(CH_3)$_3$)$_2$). ^{13}C{^{1}H} NMR (C_6D_6, 100 MHz, 298 K): δ 173.3, 153.3, 149.7, 137.3, 137.2, 132.2, 132.0, 131.6, 130.9, 130.6, 130.1, 129.9, 129.5, 127.4, 127.1, 123.9, 121.9, 119.1, 119.0 (NCHAr and all ArC), 66.1 (CH_3OAr), 33.5 (*C*(CH_3)$_3$), 31.2 (C(*C*H_3)$_3$), 5.8 (N(Si(*C*H_3)$_3$)$_2$). Anal. Calcd for $C_{60}H_{82}Br_2Mg_2N_4O_4Si_4$: C, 57.93; H, 6.64; N, 4.50. Found: C, 57.40; H, 6.60; N, 4.31.

*[(L²)₂Ca] (**2b**).* The ligand L^2H (0.373 g, 1.00 mmol) was added slowly to a solution of $Ca[N(SiMe_3)_2]_2{\cdot}2THF$ (0.507 g, 1.00 mmol) in toluene (20 mL), and the reaction solution was stirred at room temperature for 24 h. All of the volatiles were removed under vacuum. The resultant solids were recrystallized with a mixture of toluene and *n*-hexane to give yellow crystals in 55% yield (0.216 g). ^{1}H NMR (C_6D_6, 400 MHz, 298 K): δ 7.59 (s, 2H, NC*H*Ar), 7.26 (s, 2H, Ar*H*), 7.12, (br, 2H, Ar*H*), 7.04 (br, 4H, Ar*H*), 7.01−6.96 (m, 4H, Ar*H*), 6.68 (br, 4H, Ar*H*), 6.50 (s, 2H, Ar*H*), 6.23 (br, 2H, Ar*H*), 3.38 (s, 6H, CH_3OAr), 2.12 (s, 6H, CH_3Ar), 1.84 (s, 18H, C(CH_3)$_3$). ^{13}C{^{1}H} NMR (C_6D_6, 100 MHz, 298 K): δ 168.5, 159.0, 152.1, 151.9, 140.8, 134.9, 133.7, 133.0, 132.5, 132.1, 131.2, 130.5, 130.3, 129.2, 129.0, 125.0, 122.7, 121.5, 119.4 (NCHAr and all Ar*C*), 43.6 (CH_3OAr), 31.9 (*C*(CH_3)$_3$), 30.2 (C(CH_3)$_3$), 23.0 (CH_3Ar).

*[(L⁴)CaN(SiMe₃)₂·THF] (**4b**).* Following a procedure similar to that described for **1a**, L^4H (0.540 g, 1.00 mmol) was treated with $Ca[N(SiMe_3)_2]_2{\cdot}2THF$ (0.507 g, 1.00 mmol) in toluene (20 mL) at room temperature to give white solids after evaporation to dryness. Recrystallization with a mixture of toluene and *n*-hexane at −38 °C afforded yellow crystals in 56% yield (0.454 g). ^{1}H NMR (C_6D_6, 400 MHz, 298 K): δ 7.70 (s, 1H, NC*H*Ar), 7.49 (d, 1H, J = 2.1 Hz, Ar*H*), 7.42 (d, 2H, J = 7.8 Hz, Ar*H*), 7.28 (d, 2H, J = 7.8 Hz, Ar*H*), 7.17 (br, 4H, Ar*H*), 7.08−6.96 (br, 5H, Ar*H*), 6.98 (m, 2H, Ar*H*), 6.76 (m, 2H, Ar*H*), 6.68 (d, 1H, J = 7.8 Hz, Ar*H*), 6.64 (d, 1H, J = 7.8 Hz, Ar*H*), 3.57 (s, 3H, CH_3OAr), 3.02 (m, 4H, THF), 1.86 (br, 3H, C(CH_3)$_2$Ph), 1.72 (br, 3H, C(CH_3)$_2$Ph), 1.62 (s, 6H, C(CH_3)$_2$Ph), 1.02 (m, 4H THF), 0.30 (s, 18H, N(Si(CH_3)$_3$)$_2$). ^{13}C NMR (C_6D_6, 100 MHz, 298 K): δ 171.7, 168.2, 154.8, 152.9, 152.6, 151.8, 140.3, 133.4, 132.9, 132.5, 132.4, 132.0, 131.4, 130.4, 129.5, 129.3, 127.2, 126.6, 126.4, 125.8, 125.7, 125.4, 124.4, 124.1, 120.8 (NCHAr and all Ar*C*), 68.6 (THF), 64.3 (CH_3OAr), 42.7 (*C*(CH_3)$_2$Ph), 42.4 (C(CH_3)$_2$Ph), 31.9 (C(CH_3)$_2$Ph), 31.1 (C(CH_3)$_2$Ph), 25.0 (THF), 5.9 (N(Si(CH_3)$_3$)$_2$). Anal. Calcd for $C_{48}H_{62}CaN_2O_3Si_2$: C, 71.06; H, 7.70; N, 3.45. Found: C, 71.10; H, 7.99; N, 3.32.

dx.doi.org/10.1021/ic4012668 | Inorg. Chem. 2013, 52, 11821−11835

[(L⁵)₂Ca] (5b). The proligand **L⁵H** (0.602 g, 1.00 mmol) was added slowly to a solution of $Ca[N(SiMe_3)_2]_2$·2THF (0.507 g, 1.00 mmol) in toluene (20 mL), and the reaction solution was stirred at room temperature for 24 h. All of the volatiles were removed under vacuum. The resultant solids were recrystallized with a mixture of toluene and *n*-hexane to give yellow crystals in 60% yield (0.372 g). ^{1}H NMR (C_6D_6, 400 MHz, 298 K): δ 7.45−7.35 (br, 16H, Ar*H*), 7.11 (d, 2H, *J* = 7.2 Hz, toluene), 7.10−6.82 (br, 28H, Ar*H*), 6.75 (t, 3H, *J* = 7.2 Hz, toluene), 6.65−6.25 (br, 4H, Ar*H*), 6.20−5.80 (br, 4H, Ar*H*), 2.90−2.46 (br s, 6H, CH_3OAr), 2.10 (s, 3H, CH_3Tol), 1.20 (s, 18H, $C(CH_3)_3$). $^{13}C\{^1H\}$ NMR ($CDCl_3$, 100 MHz, 298 K): δ 168.7, 146.4, 145.5, 138.0, 135.0, 134.7, 131.3, 131.0, 130.9, 130.8, 128.8, 128.6, 127.0, 126.7, 124.5, 124.1, 120.7, 118.0 (NCHAr and all Ar*C*), 63.7 (CH_3OAr), 54.8 (CPh_3Ar), 33.7 ($C(CH_3)_3$), 31.3 ($C(CH_3)_3$). Anal. Calcd for $C_{86}H_{76}CaN_2O_4$·C_7H_8: C, 83.75; H, 6.35; N, 2.10. Found: C, 84.27; H, 6.45; N, 1.77.

Typical Polymerization Experiments. In a Braun Labstar glovebox, an initiator solution from a stock solution in THF or toluene was injected sequentially into a series of 10 mL vials loaded with *rac*-LA and suitable amounts of dry solvent. After specified time intervals, each vial was taken out of the glovebox; an aliquot was withdrawn and quenched quickly with wet light petroleum ether, the reaction mixture was quenched at the same time by adding an excess amount of light petroleum ether and one drop of water. All of the volatiles in the aliquots were removed, and the residue was subjected to monomer conversion determination, which was monitored by integration of monomer versus polymer methine resonances in ^{1}H NMR ($CDCl_3$, 400 MHz, 298 K). The precipitates collected from the bulk mixture were dried in air, dissolved with DCM, and sequentially precipitated into methanol. The obtained polymer was further dried in a vacuum oven at 50 °C for 16 h. Each reaction was used as one data point. In the cases where 2-propanol was used, the solution of initiator was injected into the solution of *rac*-LA and 2-propanol in toluene or THF. Otherwise, the procedures were the same.

Kinetic Studies of *rac*-LA Polymerization. A solution of the magnesium silylamido complex (0.016 mmol) in 1 mL of C_6D_6 was prepared. An NMR tube was charged with *rac*-LA (14.4 mg, 0.1 mmol), and then 0.3 mL of C_6D_6 ($[LA]_0$ = 0.2 M) and 0.2 mL of the catalyst solution were injected sequentially. The monomer conversion was continuously analyzed by ^{1}H NMR spectroscopy at room temperature.

Oligomerization Experiment. Oligomerization of *rac*-LA was carried out in C_6D_6 at 25 °C with complex **2a**·THF as the initiator under the condition of $[rac\text{-LA}]_0$:$[\mathbf{2a}\cdot\text{THF}]_0$:$[^i\text{PrOH}]_0$ = 20:1:1. The reaction mixture was stirred for 0.5 h and monitored with ^{1}H NMR spectroscopy. The mixture was then quenched by adding wet *n*-hexane. The precipitated oligomers were collected, dried under vacuum, and used for ^{1}H NMR and ESI-TOF-MS analysis.

X-ray Crystallography. Suitable crystals of complexes **2a**, **2a**·THF, **6a**, **7a**, **8a**, and **2b** for X-ray analysis were obtained from a saturated toluene/*n*-hexane mixture or a THF/*n*-hexane mixture, respectively, at −38 °C or room temperature. Diffraction data were collected on a Bruker AXSD 8 diffractometer for complexes **2a** and **2b** and a Bruker SMART APEX II diffractometer for complexes **2a**·THF, **6a**, **7a**, and **8a** with graphite-monochromated Mo Ka (λ = 0.71073 Å) radiation. All data were collected at 20 °C using the ω-scan techniques. All structures were solved by direct methods and refined using Fourier techniques. An absorption correction based on *SADABS* was applied.[36] All non-hydrogen atoms were refined by full-matrix least squares on F^2 using the *SHELXTL* program package.[37] Hydrogen atoms were located and refined by the geometry method. Cell refinement, data collection, and reduction were done by Bruker *SAINT*.[38] Structure solution and refinement were performed by *SHELXS-97*[39] and *SHELXL-97*,[40] respectively. For further crystal data and details of measurements, see Tables 2−4. Molecular structures were generated using the *ORTEP* program.[41] For complex **2a**, $C_{31}H_{44}MgN_2O_2Si_2$·C_7H_8, monoclinic, $P2(1)/c$; a = 13.546(10) Å, b = 17.057(13) Å, c = 17.275(12) Å, $\alpha = \gamma$ = 90°, β = 96.899(12)°, Z = 4. For **2a**·THF, $C_{31}H_{44}MgN_2O_2Si_2$·C_4H_8O, triclinic, $P\bar{1}$; a = 9.4272(8) Å, b = 12.9769(10) Å, c = 17.2741(14) Å, α = 100.008(2)°, β = 99.012(2)°, γ = 96.196(2)°, Z = 2. For **6a**, $C_{39.50}H_{56.50}MgN_3O_2Si_2$, triclinic, $P\bar{1}$; a = 12.8011(19) Å, b = 13.056(2) Å, c = 15.255(2) Å, α = 66.387(2)°, β = 74.955(3)°, γ = 61.162(3)°, Z = 2. For complex **7a**, $C_{60}H_{82}Cl_2Mg_2N_4O_4Si_4$, monoclinic, $P2(1)/c$; a = 16.8799(10) Å, b = 13.7086(8) Å, c = 29.2964(17) Å, $\alpha = \gamma$ = 90°, β = 101.5630(10)°, Z = 4. For complex **8a**, $C_{60}H_{82}Br_2Mg_2N_4O_4Si_4$, monoclinic, $P2(1)/c$; a = 17.023(2) Å, b = 13.7491(18) Å, c = 29.338(4) Å, $\alpha = \gamma$ = 90°, β = 101.930(2)°, Z = 4. For **2b**, $C_{60.50}H_{64.50}CaN_2O_4$, triclinic, $P\bar{1}$; a = 13.118(4) Å, b = 13.922(5) Å, c = 17.106(5) Å, α = 112.018(5)°, β = 96.288(6)°, γ = 107.016(5)°, Z = 2.

■ ASSOCIATED CONTENT

Ⓢ Supporting Information

Crystallographic data for **2a**, **2a**·THF, **6a**, **7a**, **8a**, and **2b**, ^{1}H NMR spectrum of the reaction of **L²H** and $Ca[N(SiMe_3)_2]_2$·2THF in a ratio of 1:1.5, variable-temperature ^{1}H NMR spectra of **8a** in toluene-d_8, ^{1}H NMR trace spectra of the reaction between complex **2a**, **2a**·THF, or **5a** and 2-propanol, ^{1}H NMR spectrum and ESI-TOF MS spectrum of the PLA oligomer obtained by **2a**·THF/2-propanol, homonuclear-decoupled ^{1}H NMR spectra of PLAs by complexes **5a** and **8a**, and X-ray crystallographic data of complexes **2a**, **2a**·THF, **6a**, **7a**, **8a**, and **2b** in CIF format. This material is available free of charge via the Internet at http://pubs.acs.org.

■ AUTHOR INFORMATION

Corresponding Author

*E-mail: haiyanma@ecust.edu.cn. Fax/Tel.: +86 21 64253519.

Notes

The authors declare no competing financial interest.

■ ACKNOWLEDGMENTS

This work is subsidized by the National Natural Science Foundation of China (Grant 21074032), the Program for New Century Excellent Talents in University (Grant NCET-06-0413 to H.M.), and the Fundamental Research Funds for the Central Universities (Grants WD1113011 and WK1214048). All financial support is gratefully acknowledged. H.M. also is thankful for the very kind donation of a Braun glovebox by the AvH Foundation.

■ REFERENCES

(1) (a) Drumright, R. E.; Gruber, P. R.; Henton, D. E. *Adv. Mater.* **2000**, *12*, 1841−1846. (b) Chiellini, E.; Solaro, R. *Adv. Mater.* **1996**, *8*, 305−313.

(2) (a) Platel, R. H.; Hodgson, L. M.; Williams, C. K. *Polym. Rev.* **2008**, *48*, 11−63. (b) O'Keefe, B. J.; Hillmyer, M. A.; Tolman, W. B. *J. Chem. Soc., Dalton Trans.* **2001**, 2215−2224. (c) Kamber, N. E.; Jeong, W.; Waymouth, R. M.; Pratt, R. C.; Lohmeijer, B. G. G.; Hedrick, J. L. *Chem. Rev.* **2007**, *107*, 5813−5840.

(3) (a) Spassky, H.; Wisniewski, M.; Pluta, C.; Le Borgne, A. *Macromol. Chem. Phys.* **1996**, *197*, 2627−2637. (b) Zhong, Z.; Dijkstra, P.; Feijen, J. *Angew. Chem., Int. Ed.* **2002**, *41*, 4510−4513. (c) Zhong, Z.; Dijkstra, P.; Feijen, J. *J. Am. Chem. Soc.* **2003**, *125*, 11291−11298. (d) Nomura, N.; Ishii, R.; Akakura, M.; Aoi, K. *J. Am. Chem. Soc.* **2002**, *124*, 5938−5939. (e) Alaaeddine, A.; Thomas, C. M.; Roisnel, T.; Carpentier, J.-F. *Organometallics* **2009**, *28*, 1469−1475. (f) Bouyahyi, M.; Grunova, E.; Marquet, N.; Kirillov, E.; Thomas, C. M.; Roisnel, T.; Carpentier, J.-F. *Organometallics* **2008**, *27*, 5815−5825. (g) Du, H.; Pang, X.; Yu, H.; Zhuang, X.; Chen, X.; Cui, D.; Wang, X.; Jing, X. *Macromolecules* **2007**, *40*, 1904−1913. (h) Tang, Z.; Gibson, V. C. *Eur. Polym. J.* **2007**, *43*, 150−155. (i) Qian, F.; Liu, K.; Ma, H. *Dalton Trans.* **2010**, *39*, 8071−8083. (j) Schwarz, A. D.; Chu, Z.; Mountford, P. *Organometallics* **2010**, *29*, 1246−1260. (k) Chen, H.-L.; Dutta, S.; Huang, P.-Y.; Lin, C.-C. *Organometallics* **2012**, *31*, 2016−2025.

(l) Bakewell, C.; Platel, R. H.; Cary, S. K.; Hubbard, S. M.; Roaf, J. M.; Levine, A. C.; White, A. J. P.; Long, N. J.; Haaf, M.; Williams, C. K. *Organometallics* **2012**, *31*, 4729−4736. (m) Lamberti, M.; D'Auria, I.; Mazzeo, M.; Milione, S.; Bertolasi, V.; Pappalardo, D. *Organometallics* **2012**, *31*, 5551−5560. (n) Li, G.; Lamberti, M.; Mazzeo, M.; Pappalardo, D.; Roviello, G.; Pellecchia, C. *Organometallics* **2012**, *31*, 1180−1188. (o) Normand, M.; Dorcet, V.; Kirillov, E.; Carpentier, J.-F. *Organometallics* **2013**, *32*, 1694−1709.

(4) (a) Peckermann, I.; Kapelski, A.; Spanoil, T. P.; Okuda, J. *Inorg. Chem.* **2009**, *48*, 5526−5534. (b) Pietrangelo, A.; Knight, S. C.; Gupta, A. K.; Yao, L. J.; Hillmyer, M. C.; Tolman, W. B. *J. Am. Chem. Soc.* **2010**, *132*, 11649−11657. (c) Aluthge, D. C.; Patrick, B. O.; Mehrkhodavandi, P. *Chem. Commun.* **2012**, *31*, 3499−3511.

(5) Nimitsiriwat, N.; Gibson, V. C.; Marshall, E. L.; Elsegood, M. R. J. *Inorg. Chem.* **2008**, *47*, 5417−5424.

(6) (a) Calvo, L. B.; Davidson, M. G.; García-Vivó, D. *Inorg. Chem.* **2011**, *50*, 3589−3595. (b) Lu, W.-Y.; Hsiao, M.-W.; Hsu, S. C. N.; Peng, W.-T.; Chang, Y.-J.; Tsou, Y.-C.; Wu, T.-Y.; Lai, Y.-C.; Chen, Y.; Chen, H.-Y. *Dalton Trans.* **2012**, *41*, 3659−3667.

(7) (a) Ovitt, T. M.; Coates, G. W. *J. Am. Chem. Soc.* **1999**, *121*, 4072−4073. (b) Chamberlain, B. M.; Cheng, M.; Moore, D. R.; Ovitt, T. M.; Lobkovsky, E. B.; Coates, G. W. *J. Am. Chem. Soc.* **2001**, *123*, 3229−3238. (c) Chisholm, M. H.; Gallucci, J. C.; Phomphrai, K. *Inorg. Chem.* **2005**, *44*, 8004−8010. (d) Williams, C. K.; Breyfogle, L. E.; Choi, S. K.; Nam, W.; Young, V. G.; Hillmyer, M. A.; Tolman, W. B. *J. Am. Chem. Soc.* **2003**, *125*, 11350−11359. (e) Sarazin, Y.; Liu, B.; Roisnel, T.; Maron, L.; Carpentier, J.-F. *J. Am. Chem. Soc.* **2011**, *133*, 9069−9087. (f) Wang, L.; Ma, H. *Dalton Trans.* **2010**, *39*, 7897−7910. (g) Song, S.; Zhang, X.; Ma, H.; Yang, Y. *Dalton Trans.* **2012**, *41*, 3266−3277. (h) Chuang, H.-J.; Weng, S.-F.; Chang, C.-C.; Lin, C.-C.; Chen, H.-Y. *Dalton Trans.* **2011**, *40*, 9601−9607. (i) Börner, J.; Vieira, I. S.; Pawlis, A.; Döring, A.; Kuckling, D.; Herres-Pawlis, S. *Chem.—Eur. J.* **2011**, *17*, 4507−4512. (j) Darensbourg, D. J.; Karroonnirun, O. *Inorg. Chem.* **2010**, *49*, 2360−2371. (k) Yang, N.; Xin, L.; Gao, W.; Zhang, J.; Luo, X.; Liu, X.; Mu, Y. *Dalton Trans.* **2012**, *41*, 11454−11463. (l) D'Auria, I.; Lamberti, M.; Mazzeo, M.; Milione, S.; Roviello, G.; Pellecchia, C. *Chem.—Eur. J.* **2012**, *18*, 2349−2360.

(8) (a) Garcés, A.; Sánchez-Barba, L. F.; Alonso-Moreno, C.; Fajardo, M.; Fernández-Baeza, J.; Otero, A.; Lara-Sánchez, A.; López-Solera, I.; Rodríguez, A. M. *Inorg. Chem.* **2010**, *49*, 2859−2871. (b) Fedushkin, I. L.; Morozov, A. G.; Chudakova, V. A.; Fukin, G. K.; Cherkasov, V. K. *Eur. J. Inorg. Chem.* **2009**, *48*, 4995−5003. (c) Grala, A.; Ejfler, J.; Jerzykiewicz, L. B.; Sobota, P. *Dalton Trans.* **2011**, *40*, 4042−4044. (d) Wang, L.; Ma, H. *Macromolecules* **2010**, *43*, 6535−6537. (e) Chen, M.-T.; Chang, P.-J.; Huang, C.-A.; Peng, K.-F.; Chen, C.-T. *Dalton Trans.* **2009**, *38*, 9068−9074. (f) Chen, H.-Y.; Mialon, L.; Abboud, K. A.; Miller, S. A. *Organometallics* **2012**, *31*, 5252−5261. (g) Sung, C.-Y.; Li, C.-Y.; Su, J.-K.; Chen, T.-Y.; Lin, C.-H.; Ko, B.-T. *Dalton Trans.* **2012**, *41*, 953−961. (h) Wang, Y.; Zhao, W.; Liu, D.; Li, S.; Liu, X.; Cui, D.; Chen, X. *Organometallics* **2012**, *31*, 4182−4190.

(9) (a) Darensbourg, D. J.; Choi, W.; Karroonnirun, O.; Bhuvanesh, N. *Macromolecules* **2008**, *41*, 3493−3502. (b) Chen, H.-Y.; Tang, H.-Y.; Lin, C.-C. *Polymer* **2007**, *48*, 2257−2262. (c) Avent, A. G.; Crimmin, M. R.; Hill, M. S.; Hitchcock, P. B. *Organometallics* **2005**, *24*, 1184−1188. (d) Davin, J. P.; Buffet, J.-C.; Spaniol, T. P.; Okuda, J. *Dalton Trans.* **2012**, *41*, 12612−12618. (e) Liu, B.; Roisnel, T.; Guégan, J.-P.; Carpentier, J.-F.; Sarazin, Y. *Chem.—Eur. J.* **2012**, *18*, 6289−6301. (f) Liu, B.; Dorcet, V.; Maron, L.; Carpentier, J.-F.; Sarazin, Y. *Eur. J. Inorg. Chem.* **2012**, 3023−3031.

(10) (a) Sergeeva, E.; Kopilov, J.; Goldberg, I.; Kol, M. *Inorg. Chem.* **2010**, *49*, 3977−3979. (b) Romain, C.; Brelot, L.; Bellemin-Laponnaz, S.; Dagorne, S. *Organometallics* **2010**, *29*, 1191−1198. (c) Gendler, S.; Segal, S.; Goldberg, I.; Goldschmidt, Z.; Kol, M. *Inorg. Chem.* **2006**, *45*, 4783−4790. (d) Chmura, A. J.; Davidson, M. G.; Frankis, C. J.; Jones, M. D.; Lunn, M. D. *Chem. Commun.* **2008**, *44*, 1293−1295. (e) Whitelaw, E. L.; Jones, M. D.; Mahon, M. F.; Kociok-Kohn, G. *Dalton Trans.* **2009**, *38*, 9020−9025. (f) Saha, T. K.; Rajashekhar, B.; Gowda, R. R.; Ramkumar, V.; Chakraborty, D. *Dalton Trans.* **2010**, *39*, 5091−5093. (g) Schwarz, A. D.; Thompson, A. L.; Mountford, P. *Inorg. Chem.* **2009**, *48*, 10442−10454. (h) Whitelaw, E. L.; Davidson, M. D.; Jones, M. D. *Chem. Commun.* **2011**, *47*, 10004−10006. (i) Sauer, A.; Buffet, J.-C.; Spaniol, T. P.; Nagae, H.; Mashima, K.; Okuda, J. *Inorg. Chem.* **2012**, *51*, 5764−5770. (j) Stopper, A.; Okuda, J.; Kol, M. *Macromolecules* **2012**, *45*, 698−704. (k) Li, C.-Y.; Yu, C.-J.; Ko, B.-T. *Organometallics* **2013**, *32*, 172−180.

(11) (a) Ma, H.; Spaniol, T. P.; Okuda, J. *Dalton Trans.* **2003**, 4770−4780. (b) Ma, H.; Okuda, J. *Macromolecules* **2005**, *38*, 2665−2673. (c) Ma, H.; Spaniol, T. P.; Okuda, J. *Angew. Chem., Int. Ed.* **2006**, *45*, 7818−7821. (d) Nie, K.; Gu, X.; Yao, Y.; Zhang, Y.; Shen, Q. *Dalton Trans.* **2010**, *39*, 6832−6840. (e) Yang, S.; Zhu, D.; Zhang, Y.; Shen, Q. *Chem. Commun.* **2012**, *48*, 9780−9782. (f) Bakewell, C.; Cao, T.-P.-A.; Long, N.; Goff, X. F. L.; Auffrant, A.; Williams, C. K. *J. Am. Chem. Soc.* **2012**, *134*, 20577−20580. (g) Kratsch, J.; Kuzdrowska, M.; Schmid, M.; Kazeminejad, N.; Kaub, C.; Oña-Burgos, P.; Guillaume, S. M.; Roesky, P. W. *Organometallics* **2013**, *32*, 1230−1238. (h) Nie, K.; Gu, W.; Yao, Y.; Zhang, Y.; Shen, Q. *Organometallics* **2013**, *32*, 2608−2617. (i) Cao, T.-P.-A.; Buchard, A.; Goff, F. L.; Auffrant, A.; Williams, C. K. *Inorg. Chem.* **2012**, *51*, 2157−2169.

(12) Frazza, E. J.; Schmitt, E. E. J. *Biomed. Mater. Res. Symp.* **1971**, *1*, 43−58.

(13) (a) Jerome, C.; Lecomte, P. *Adv. Drug Delivery Rev.* **2008**, *60*, 1056−1076. (b) Penczek, S.; Cypryk, M.; Duda, A.; Kubisa, P.; Slomkowski, S. *Prog. Polym. Sci.* **2007**, *32*, 247−282.

(14) (a) Chisholm, M. H.; Iyer, S. S.; McCollum, D. G.; Pagel, M.; Werner-Zwanziger, U. *Macromolecules* **1999**, *32*, 963−973. (b) Hubbell, J. A.; Langer, R. *Chem. Eng. News* **1995**, *73*, 42−54. (c) Langer, R.; Vacanti, J. P. *Science* **1993**, *260*, 920−926.

(15) Chen, C.-M.; Huang, J.-S. *Coord. Chem. Rev.* **2003**, *242*, 97−113 and references cited therein.

(16) Wu, J.-C.; Huang, B.-H.; Hsueh, M.-L.; Lai, S.-L.; Lin, C.-C. *Polymer* **2005**, *46*, 9784−9792.

(17) Hung, W.-C.; Lin, C.-C. *Inorg. Chem.* **2009**, *48*, 728−734.

(18) (a) Lin, C. F.; Ojima, I. *J. Org. Chem.* **2011**, *76*, 6240−6249. (b) Dubovyk, I.; Watson, I. D. G.; Yudin, A. K. *J. Am. Chem. Soc.* **2007**, *129*, 14172−14173. (c) Sun, X.; Zhou, L.; Li, W.; Zhang, X. *J. Org. Chem.* **2008**, *73*, 1143−1146. (d) Nelson, S. G.; Hilfiker, M. A. *Org. Lett.* **1999**, *1*, 1379−1382. (e) Qiu, L.; Qi, J.; Pai, C.-C.; Chan, S.; Zhou, Z.; Choi, M. C. K.; Chan, A. S. C. *Org. Lett.* **2002**, *4*, 4599−4602. (f) Kuethe, J. T.; Wong, A.; Wu, J.; Davies, I. W.; Dormer, P. G.; Welch, C. J.; Hillier, M. C.; Hughes, D. L.; Reider, P. J. *J. Org. Chem.* **2002**, *67*, 5993−6000. (g) Fabris, F.; Lucchi, O. D. *J. Org. Chem.* **1997**, *62*, 7156−7164.

(19) Suzuki, Y.; Kinoshita, S.; Shibahara, A.; Ishii, S.; Kawamura, K.; Inoue, Y.; Fujita, T. *Organometallics* **2010**, *29*, 2394−2396.

(20) (a) Chisholm, M. H.; Gallucci, J. C.; Phomphrai, K. *Inorg. Chem.* **2005**, *44*, 8004−8010. (b) Hsueh, L.-F.; Chuang, N.-T.; Lee, C.-Y.; Datta, A.; Huang, J.-H.; Lee, T.-Y. *Eur. J. Inorg. Chem.* **2011**, *36*, 5530−5537. (c) Range, S.; Piesik, D. F.-J.; Harder, S. *Eur. J. Inorg. Chem.* **2008**, *14*, 3442−3451. (d) Allan, J. F.; Henderson, K. W.; Kennedy, A. R. *Chem. Commun.* **1999**, 1325−1326. (e) Sebestl, J. L.; Nadasdi, T. T.; Heeg, M. J.; Winter, C. H. *Inorg. Chem.* **1998**, *37*, 1289−1294.

(21) (a) Wang, Q.; Xiang, L.; Song, H.; Zi, G. *Inorg. Chem.* **2008**, *47*, 4319−4328. (b) Perkins, J. R.; Carter, R. G. *J. Am. Chem. Soc.* **2008**, *130*, 3290−3291. (c) Li, X.; Meng, X.; Su, H.; Wu, X.; Xu, D. *Synlett* **2008**, *6*, 857−860.

(22) (a) Sedai, B.; Heeg, M. J.; Winter, C. H. *J. Organomet. Chem.* **2008**, *693*, 3495−3503. (b) Teng, W.; Guino-o, M.; Hitzbleck, J.; Englich, U.; Ruhlandt-Senge, K. *Inorg. Chem.* **2006**, *45*, 9531−9539. (c) Zheng, Z.; Elmkaddem, M. K.; Fischmeister, C.; Roisnel, T.; Thomas, C. M.; Carpentier, J.-F.; Renaud, J.-L. *New J. Chem.* **2008**, *32*, 2150−2158.

(23) There is a 30% possibility of having *R,R* or *S,S* configuration of the two biphenyl moieties in one molecule.

(24) Tang, H.-Y.; Chen, H.-Y.; Huang, J.-H.; Lin, C.-C. *Macromolecules* **2007**, *40*, 8855−8860.

(25) Chisholm, M. H.; Gallucci, J. C.; Phomphrai, K. *Inorg. Chem.* **2004**, *43*, 6717−6725.

(26) The bisligated magnesium complex $(\mathbf{L^2})_2$Mg could be obtained from the reaction of $\{Mg[N(SiMe_3)_2]_2\}_2$ and proligand $\mathbf{L^2H}$ in a 1:2 ratio. ^{1}H NMR (C_6D_6, 400 MHz, 298 K): δ 7.68 (s, 2H, NC*H*Ar), 7.30 (d, 2H, J = 2.2 Hz, Ar*H*), 7.03 (td, 2H, J = 7.5 and 1.0 Hz, Ar*H*), 6.93 (t, 2H, J = 7.5 Hz, Ar*H*), 6.86 (t, 2H, J = 6.8 Hz, Ar*H*), 7.0−6.70 (br, 4H, Ar*H*, overlapped with other signals), 6.58 (br, 2H, Ar*H*), 6.50 (d, 2H, J = 2.2 Hz, Ar*H*), 6.50−6.10 (br, 4H, Ar*H*), 3.19 (s, 6H, C*H*$_3$OAr), 2.15 (s, 6H, C*H*$_3$Ar), 1.75 (s, 18H, C(C*H*$_3$)$_3$).
(27) Amgoune, A.; Thomas, C. M.; Roisnel, T.; Carpentier, J.-F. *Chem.—Eur. J.* **2006**, *12*, 169−179.
(28) Chisholm, M. H.; Choojun, K.; Gallucci, J. C.; Wambua, P. M. *Chem. Sci.* **2012**, *3*, 3445−3457.
(29) Marshall, E. L.; Gibson, V. C.; Rzepa, H. S. *J. Am. Chem. Soc.* **2005**, *127*, 6048−6051.
(30) Westerhausen, M. *Inorg. Chem.* **1991**, *30*, 96−101.
(31) Sarazin, Y.; Howard, R. H.; Hughes, D. L.; Humphrey, S. M.; Bochmann, M. *Dalton Trans.* **2006**, 340−350.
(32) Casiraghi, G.; Casnati, G.; Puglia, G.; Sartori, G.; Terenghi, G. *J. Chem. Soc., Perkin Trans. 1* **1980**, 1862−1865.
(33) Kochnev, A. I.; Oleynik, I. I.; Oleynik, I. V.; Ivanchev, S. S.; Tolstikov, G. A. *Russ. Chem. Bull., Int. Ed.* **2007**, *56* (6), 1125−1129.
(34) (a) Masilamani, D.; Rogic, M. M. *J. Org. Chem.* **1981**, *46*, 4486−4489. (b) Forgan, R. S.; Roach, B. D.; Wood, P. A.; White, F. J.; Campbell, J.; Henderson, D. K.; Kamenetzky, E.; McAllister, F. E.; Parsons, S.; Pidcock, E.; Richardson, P.; Swart, R. M.; Tasker, P. A. *Inorg. Chem.* **2011**, *50*, 4515−4522.
(35) Lam, F.; Xu, J.; Chan, K. *J. Org. Chem.* **1996**, *61*, 8414−8418.
(36) *SADABS, Bruker Nonius area detector scaling and absorption correction*, version 2.05; Bruker AXS Inc.: Madison, WI, 1996.
(37) Sheldrick, G. M. *SHELXTL 5.10 for windows NT, Structure Determination Software Programs*; Bruker AXS Inc.: Madison, WI, 1997.
(38) *SAINT*, version *6.02*; Bruker AXS Inc.: Madison WI, 1999; pp 53711−5373.
(39) Sheldrick, G. M. *SHELXS-97, Program for the Solution of Crystal Structures*; University of Göttingen: Göttingen, Germany, 1990.
(40) Sheldrick, G. M. *SHELXL-97, Program for the Refinement of Crystal Structures*; University of Göttingen: Göttingen, Germany, 1997.
(41) ORTEP-III for Windows, version 2.0: Farrugia, L. J. *J. Appl. Crystallogr.* **1997**, *30*, 565.